

Quantum Knots and New Quantum Field Theory

Sze Kui Ng

Department of Mathematics, City University of Hong Kong, Hong Kong

Abstract

We propose a new quantum gauge field of electrodynamics (QED) and chromodynamics (QCD) from which we construct quantum knots and derive knot invariants such as the Jones polynomial. Our approach is inspired by the work of Witten who derived knot invariants from quantum field theory based on the Chern-Simon Lagrangian. From our approach we can derive new knot invariants which extend the Jones polynomial and give a complete classification of knots. Then we model elementary particles by quantum knots. From the construction of quantum knots we construct quantum photon propagator and quantum gluon propagator for the nuclear force between elementary particles. Then from the propagators a renormalization group equation is derived for the critical phenomena of QED and QCD.

1 Introduction

In 1989 Witten derived knot invariants such as the Jones polynomial from quantum field theory based on the Chern-Simon Lagrangian [1]. Inspired by Witten's work in this paper we shall derive quantum knots and knot invariants from a new quantum gauge field of electrodynamics (QED) and chromodynamics (QCD). In our approach we shall first construct quantum knots and their knot invariants and then derive the Jones polynomial.

Then we model elementary particles by quantum knots. From the construction of quantum knots we construct quantum photon propagator and quantum gluon propagator for the nuclear force between elementary particles. Then from the propagators a renormalization group equation is derived for the critical phenomena of QED and QCD. Then from this renormalization group equation for the critical phenomena we derive a model of superconductivity for electrons and a model of superfluid and color superconductivity for quarks in neutron stars.

This paper is organized as follows. From section 2 to section 9 we give a brief description of a new quantum gauge field theory of QED and QCD. From this gauge theory we derive two quantum Knizhnik-Zamolodchikov equations. From these two KZ equations we derive a quantum group structure for the product of Wilson lines. When the products of Wilson lines form closed curves they are as quantum knots. From product of Wilson lines and quantum knots we derive new knot invariants which extend the Jones polynomial and give a classification of knots.

Then from section 10 to section 11 the quantum knot based on the $U(1)$ group is as the model of photon and quantum knots based on $SU(2)$ and $SU(3)$ are as gluons. When the quantum knots act on complex vectors representing spinors (for electrons or quarks) this gives models of electron, mesons and baryons. Then the quantum Wilson line is as a gluon propagator connecting elementary particle represented by quantum knots at z_0 to elementary particle represented by quantum knots at z . When the gauge group is $U(1)$ it is as the photon propagator. We show that the quantum gluon propagator gives properties of nuclear force (or strong interaction) that it is strong in the short distance and is weak in the long distance between the elementary particles and is with the property of asymptotic freedom.

Then from section 12 to section 18 with the gluon propagator and the photon propagator we derive critical phenomena of electrons and quarks including superconductivity and color superconductivity.

2 New gauge model of QED and QCD

Let us first describe a new quantum field theory. Similar to the Wiener measure for the Brownian motion which is constructed from the integral $\int_{t_0}^{t_1} \left(\frac{dx}{dt}\right)^2 dt$ we construct a measure for QED from the following energy integral:

$$- \int_{s_0}^{s_1} Dds := - \int_{s_0}^{s_1} \left[\frac{1}{2} \left(\frac{\partial A_1}{\partial x^2} - \frac{\partial A_2}{\partial x^1} \right)^* \left(\frac{\partial A_1}{\partial x^2} - \frac{\partial A_2}{\partial x^1} \right) + \left(\frac{dZ^*}{ds} + ie_0 AZ^* \right) \left(\frac{dZ}{ds} - ie_0 AZ \right) \right] ds \quad (1)$$

where the complex variable $Z = Z(z(s))$ and the real variables $A_1 = A_1(z(s))$ and $A_2 = A_2(z(s))$ are continuous functions in a form that they are in terms of a (continuously differentiable) curve $z(s) = C(s) = (x^1(s), x^2(s))$, $s_0 \leq s \leq s_1$, $z(s_0) = z(s_1)$ in the complex plane where s is a parameter representing the proper time in relativity (We shall also write $z(s)$ in the complex variable form $C(s) = z(s) = x^1(s) + ix^2(s)$, $s_0 \leq s \leq s_1$). The complex variable $Z = Z(z(s))$ represents a field of matter (such as the electron) (Z^* denotes its complex conjugate) and the real variables $A_1 = A_1(z(s))$ and $A_2 = A_2(z(s))$ represent a connection (or the gauge field of the photon), and $A = \sum_{j=1}^2 A_j \frac{dx^j}{ds}$, and e_0 denotes the (bare) electric charge.

The integral (1) has the following gauge symmetry:

$$Z'(z(s)) := Z(z(s))e^{ie_0 a(z(s))}, \quad A'_j(z(s)) := A_j(z(s)) + \frac{\partial a}{\partial x^j} \quad j = 1, 2 \quad (2)$$

where $a = a(z)$ is a continuously differentiable real-valued function of z .

Similar to the usual Yang-Mills gauge theory we can generalize this gauge theory with $U(1)$ gauge symmetry to nonabelian gauge theories. As an illustration let us consider the gauge symmetry $SU(2) \otimes U(1)$ for the model of QCD where $SU(2) \otimes U(1)$ denotes the direct product of the groups $SU(2)$ and $U(1)$. Similar to (1) we consider the following energy integral:

$$L := \int_{s_0}^{s_1} \left[\frac{1}{2} Tr(D_1 A_2 - D_2 A_1)^* (D_1 A_2 - D_2 A_1) + (D_0^* Z^*) (D_0 Z) \right] ds \quad (3)$$

where $Z = (z_1, z_2)^T$ is a two dimensional complex vector; $A_j = \sum_{k=0}^3 A_j^k t^k$ ($j = 1, 2$) where A_j^k denotes a component of a gauge field A^k ; $t^k = iT^k$ denotes a generator of $SU(2) \otimes U(1)$ where T^k denotes a self-adjoint generator of $SU(2) \otimes U(1)$ (here for simplicity we choose a convention that the complex i is absorbed by t^k and t^k is absorbed by A_j ; and the notation A_j is with a little confusion with the notation A_j in the above formulation of (1) where A_j , $j = 1, 2$ are real valued); and $D_i = \frac{\partial}{\partial x^i} - e_0$ for $i = 1, 2$ where $A = \sum_{j=1}^2 A_j \frac{dx^j}{ds}$; and $D_0 = \frac{d}{ds} - e_0 A$ where e_0 is the bare electric charge for general interactions including the strong and weak interactions.

We have that (3) is invariant under the following gauge transformation:

$$\begin{aligned} Z'(z(s)) &:= U(a(z(s)))Z(z(s)) \\ A'_j(z(s)) &:= U(a(z(s)))A_j(z(s))U^{-1}(a(z(s))) + U(a(z(s)))\frac{\partial U^{-1}}{\partial x^j}(a(z(s))), j = 1, 2 \end{aligned} \quad (4)$$

where $U(a(z(s))) = e^{a(z(s))}$; $a(z(s)) = \sum_k e_0 a^k(z(s))t^k$ for some functions a^k . We shall mainly consider the case that a is a function of the form $a(z(s)) = \sum_k \text{Re } \omega^k(z(s))t^k$ where ω^k are analytic functions of z (We let $\omega(z(s)) := \sum_k \omega^k(z(s))t^k$ and we write $a(z) = \text{Re } \omega(z)$).

Similarly we have a model of QCD based on the gauge symmetry $SU(3) \times U(1)$.

The above gauge theory is based on the Banach space X of continuous functions $Z(z(s))$, $A_j(z(s))$, $j = 1, 2$, $s_0 \leq s \leq s_1$ on the one dimensional interval $[s_0, s_1]$. Since L is positive and the theory is one dimensional (and thus is simpler than the usual two dimensional Yang-Mills gauge theory) we have that this gauge theory is similar to the Wiener measure except that this gauge theory has a gauge symmetry.

3 Dirac-Wilson loop

Similar to the Wilson loop in quantum field theory [1], from our quantum theory we introduce an analogue of Wilson loop, as follows (We shall also call a Wilson loop as a Dirac-Wilson loop).

Definition. A classical Wilson loop $W_R(C)$ is defined by :

$$W_R(C) := P e^{\int_C A_j dx^j} \quad (5)$$

where R denotes a representation of $SU(2)$; $C(\cdot) = z(\cdot)$ is a fixed closed curve where the quantum gauge theories are based on it as specific in the above section. As usual the notation P in the definition of $W_R(C)$ denotes a path-ordered product [1][4][5].

When the curve $C(\cdot) = z(\cdot)$ is not a closed curve, we call $W_R(C)$ as a classical Wilson line.

Let z_0 and z_1 denotes the end points of $C(\cdot) = z(\cdot)$. Then, in [9], we show that, based on the above quantum gauge model with the gauge invariance property, the quantum version of $W_R(C)$, denoted by $W(z_0, z_1)$, satisfies the following quantum Knizhnik-Zamolodchikov equation [9, 10, 11, 12]:

$$\partial_{z_i} W(z_1, z'_1) \cdots W(z_n, z'_n) = \frac{-e_0^2}{k_0 + g_0} \sum_{j \neq i}^n \frac{\sum_a t_i^a \otimes t_j^a}{z_i - z_j} W(z_1, z'_1) \cdots W(z_n, z'_n), \quad (6)$$

for $i = 1, \dots, n$ where g_0 denotes the dual Coxeter number of a group multiplying with e_0^2 and we have $g_0 = 2e_0^2$ for the group $SU(2)$ (When the gauge group is $U(1)$ we have $g_0 = 0$). We remark that in (6) we have defined $t_i^a := t^a$ and:

$$t_i^a \otimes t_j^a W(z_1, z'_1) \cdots W(z_n, z'_n) := W(z_1, z'_1) \cdots [t^a W(z_i, z'_i)] \cdots [t^a W(z_j, z'_j)] \cdots W(z_n, z'_n). \quad (7)$$

The above quantum Knizhnik-Zamolodchikov equation is with respect to the left side variables z_i . It is interesting that we also have the following quantum Knizhnik-Zamolodchikov equation with respect to the right side z'_i variables which is dual to (6):

$$\partial_{z'_i} W(z_1, z'_1) \cdots W(z_n, z'_n) = \frac{-e_0^2}{k_0 + g_0} \sum_{j \neq i}^n W(z_1, z'_1) \cdots W(z_n, z'_n) \frac{\sum_a t_i^a \otimes t_j^a}{z'_j - z'_i} \quad (8)$$

for $i = 1, \dots, n$ where we have defined:

$$W(z_1, z'_1) \cdots W(z_n, z'_n) t_i^a \otimes t_j^a := W(z_1, z'_1) \cdots [W(z_i, z'_i) t^a] \cdots [W(z_j, z'_j) t^a] \cdots W(z_n, z'_n). \quad (9)$$

4 Solving quantum KZ equation

Let us consider the following product of two quantum Wilson lines:

$$G(z_1, z_2, z_3, z_4) := W(z_1, z_2) W(z_3, z_4) \quad (10)$$

where the two quantum Wilson lines $W(z_1, z_2)$ and $W(z_3, z_4)$ represent two pieces of curves starting at z_1 and z_3 and ending at z_2 and z_4 respectively. We have that this product G satisfies the KZ equation for the variables z_1, z_3 and satisfies the dual KZ equation for the variables z_2 and z_4 . Then by solving the two-variables-KZ equation in (6) we have that a form of G is given by [6][7][8]:

$$e^{-\hat{t} \log[\pm(z_1 - z_3)]} C_1 \quad (11)$$

where $\hat{t} := \frac{e_0^2}{k_0 + g_0} \sum_a t^a \otimes t^a$ and C_1 is a constant matrix which is independent of the variable $z_1 - z_3$. We see that G is a multi-valued analytic function where the determination of the \pm sign depended on the choice of the branch. Then by solving the dual two-variable-KZ equation in (8) we have that G is of the form:

$$C_2 e^{\hat{t} \log[\pm(z_4 - z_2)]} \quad (12)$$

where C_2 is a constant matrix which is independent of the variable $z_4 - z_2$. From (11), (12) and letting:

$$C_1 = A e^{\hat{t} \log[\pm(z_4 - z_2)]}, \quad C_2 = e^{-\hat{t} \log[\pm(z_1 - z_3)]} A \quad (13)$$

where A is an initial operator we have that G is given by

$$G(z_1, z_2, z_3, z_4) = e^{-\hat{t} \log[\pm(z_1 - z_3)]} A e^{\hat{t} \log[\pm(z_4 - z_2)]} \quad (14)$$

where at the singular case that $z_1 = z_3$ we simply define $\log[\pm(z_1 - z_3)] = 0$. Similarly for $z_2 = z_4$.

5 Computation of quantum Wilson lines and loops

Let us consider the following product of two quantum Wilson lines:

$$G(z_1, z_2, z_3, z_4) := W(z_1, z_2)W(z_3, z_4) \quad (15)$$

where the two quantum Wilson lines $W(z_1, z_2)$ and $W(z_3, z_4)$ represent two pieces of curves starting at z_1 and z_3 and ending at z_2 and z_4 respectively. As shown in the above section we have that G is given by the following formula:

$$G(z_1, z_2, z_3, z_4) = e^{-\hat{t} \log[\pm(z_1-z_3)]} A e^{\hat{t} \log[\pm(z_4-z_2)]} \quad (16)$$

where the product is a 4-tensor. Let us set $z_2 = z_3$. Then the 4-tensor $W(z_1, z_2)W(z_3, z_4)$ is reduced to the 2-tensor $W(z_1, z_2)W(z_2, z_4)$. By using (16) the 2-tensor $W(z_1, z_2)W(z_2, z_4)$ is given by:

$$W(z_1, z_2)W(z_2, z_4) = e^{-\hat{t} \log[\pm(z_1-z_2)]} A_{14} e^{\hat{t} \log[\pm(z_4-z_2)]} \quad (17)$$

where $A_{14} = A_1 \otimes A_4$ is a 2-tensor reduced from the 4-tensor $A = A_1 \otimes A_2 \otimes A_3 \otimes A_4$ in (16). In this reduction the \hat{t} operator of $\Phi = e^{-\hat{t} \log[\pm(z_1-z_2)]}$ acting on the left side of A_1 and A_3 in A is reduced to acting on the left side of A_1 and A_4 in A_{14} . Similarly the \hat{t} operator of $\Psi = e^{-\hat{t} \log[\pm(z_4-z_2)]}$ acting on the right side of A_2 and A_4 in A is reduced to acting on the right side of A_1 and A_4 in A_{14} .

Then since \hat{t} is a 2-tensor operator we have that \hat{t} is as a matrix acting on the two sides of the 2-tensor A_{14} which is also as a matrix with the same dimension as \hat{t} . Thus Φ and Ψ are as matrices of the same dimension as the matrix A_{14} acting on A_{14} by the usual matrix operation. Then since \hat{t} is a Casimir operator for the 2-tensor group representation of $SU(2)$ we have that Φ and Ψ commute with A_{14} since Φ and Ψ are exponentials of t (We remark that Φ and Ψ are in general not commute with the 4-tensor initial operator A). Thus we have

$$e^{-\hat{t} \log[\pm(z_1-z_2)]} A_{14} e^{\hat{t} \log[\pm(z_4-z_2)]} = e^{-\hat{t} \log[\pm(z_1-z_2)]} e^{\hat{t} \log[\pm(z_4-z_2)]} A_{14} \quad (18)$$

Let us set $z_1 = z_4$. In this case the quantum Wilson line forms a closed loop. Now in (18) with $z_1 = z_4$ we have that $e^{-\hat{t} \log[\pm(z_1-z_2)]}$ and $e^{\hat{t} \log[\pm(z_1-z_2)]}$ which come from the two-side KZ equations cancel each other and from the multi-valued property of the log function we have

$$W(z_1, z_1) = R^N A_{14} \quad N = 0, \pm 1, \pm 2, \dots \quad (19)$$

where $R = e^{-i\pi\hat{t}}$ is the monodromy of the KZ equation [6].

6 Representing braiding of curves by quantum Wilson Lines

Consider again the product $G(z_1, z_2, z_3, z_4) = W(z_1, z_2)W(z_3, z_4)$. We have that G is a multivalued analytic function where the determination of the \pm sign depended on the choice of the branch.

Let the two pieces of curves be crossing at w . Then we have $W(z_1, z_2) = W(z_1, w)W(w, z_2)$ and $W(z_3, z_4) = W(z_3, w)W(w, z_4)$. Thus we have

$$W(z_1, z_2)W(z_3, z_4) = W(z_1, w)W(w, z_2)W(z_3, w)W(w, z_4) \quad (20)$$

If we interchange z_1 and z_3 , then from (20) we have the following ordering:

$$W(z_3, w)W(w, z_2)W(z_1, w)W(w, z_4) \quad (21)$$

Now let us choose a branch. Suppose that these two curves are cut from a knot and that following the orientation of a knot the curve represented by $W(z_1, z_2)$ is before the curve represented by $W(z_3, z_4)$. Then we fix a branch such that the product in (16) is with two positive signs :

$$W(z_1, z_2)W(z_3, z_4) = e^{-t \log(z_1-z_3)} A e^{t \log(z_4-z_2)} \quad (22)$$

Then if we interchange z_1 and z_3 we have

$$W(z_3, w)W(w, z_2)W(z_1, w)W(w, z_4) = e^{-t \log[-(z_1 - z_3)]} A e^{t \log(z_4 - z_2)} \quad (23)$$

From (22) and (23) as a choice of branch we have

$$W(z_3, w)W(w, z_2)W(z_1, w)W(w, z_4) = RW(z_1, w)W(w, z_2)W(z_3, w)W(w, z_4) \quad (24)$$

where $R = e^{-i\pi t}$ is the monodromy of the KZ equation. In (24) z_1 and z_3 denote two points on a closed curve such that along the direction of the curve the point z_1 is before the point z_3 and in this case we choose a branch such that the angle of $z_3 - z_1$ minus the angle of $z_1 - z_3$ is equal to π .

Now from (24) we can take a convention that the ordering (21) represents that the curve represented by $W(z_1, z_2)$ is upcrossing the curve represented by $W(z_3, z_4)$ while (20) represents zero crossing of these two curves.

Similarly from the dual KZ equation as a choice of branch which is consistent with the above formula we have

$$W(z_1, w)W(w, z_4)W(z_3, w)W(w, z_2) = W(z_1, w)W(w, z_2)W(z_3, w)W(w, z_4)R^{-1} \quad (25)$$

where z_2 is before z_4 . We take a convention that the ordering (25) represents that the curve represented by $W(z_1, z_2)$ is undercrossing the curve represented by $W(z_3, z_4)$. Here along the orientation of a closed curve the piece of curve represented by $W(z_1, z_2)$ is before the piece of curve represented by $W(z_3, z_4)$. In this case since the angle of $z_3 - z_1$ minus the angle of $z_1 - z_3$ is equal to π we have that the angle of $z_4 - z_2$ minus the angle of $z_2 - z_4$ is also equal to π and this gives the R^{-1} in this formula (25).

From (24) and (25) we have

$$W(z_3, z_4)W(z_1, z_2) = RW(z_1, z_2)W(z_3, z_4)R^{-1} \quad (26)$$

where z_1 and z_2 denote the end points of a curve which is before a curve with end points z_3 and z_4 . From (26) we see that the algebraic structure of these quantum Wilson lines $W(z, z')$ is analogous to the quasi-triangular quantum group [11][6].

7 Skein relation for the HOMFLY polynomial

In this section let us apply the above result which is from the KZ equation in dual form to derive the skein relation for the HOMFLY polynomial which includes the Jones polynomial. From this relation we then have the skein relation for the Jones polynomial which is a special case of the HOMFLY polynomial [4][13][14].

It is well known that from the one-side KZ equation we can derive a braid group representation which is related to the derivation of the skein relation for the Jones polynomial [7][8]. We shall see here that by applying the two KZ equations of the KZ equation in dual form we also have a way to derive the skein relation for the HOMFLY polynomial.

Let us first consider the following theorem of Kohno and Drinfeld [6][7][8]:

Theorem 1 (Kohno-Drinfeld) *Let R be the monodromy of the KZ equation for the group $SU(2)$ and let \bar{R} denotes the R -matrix of the quantum group $U_q(su(2))$ where $su(2)$ denotes the Lie algebra of $SU(2)$ and $q = e^{\frac{i2\pi}{k+g}}$ where $g = 2$. Then there exists a twisting $F \in U_q(su(2)) \otimes U_q(su(2))$ such that*

$$\bar{R} = F^{-1}RF^{-1} \quad (27)$$

From this relation we have that the braid group representations obtained from the quantum group $U_q(su(2))$ and obtained from the one-side KZ equation are equivalent.

We shall use only the relation (27) of this theorem to derive the skein relation of the HOMFLY polynomial. From the property of the quantum group $U_q(su(2))$ we also have the following formula

$$\bar{R}^2 - (q^{\frac{1}{2}} - q^{-\frac{1}{2}})\bar{R} - I = 0 \quad (28)$$

Thus we have

$$\bar{R} - (q^{\frac{1}{2}} - q^{-\frac{1}{2}})I - \bar{R}^{-1} = 0 \quad (29)$$

By using this formula we have

$$[\bar{R} - (q^{\frac{1}{2}} - q^{-\frac{1}{2}})I - \bar{R}^{-1}]FW(z_1, w)W(w, z_2)W(z_3, w)W(w, z_4)F^{-1} = 0 \quad (30)$$

Thus by using the relation (27) we have

$$\begin{aligned} & TrF^{-1}RW(z_1, w)W(w, z_2)W(z_3, w)W(w, z_4)F^{-1} \\ & - (q^{\frac{1}{2}} - q^{-\frac{1}{2}})TrFW(z_1, z_2)W(z_3, z_4)F^{-1} \\ & - TrFW(z_1, w)W(w, z_2)W(z_3, w)W(w, z_4)R^{-1}F = 0 \end{aligned} \quad (31)$$

Then by using the formulas (24) and (25) for upcrossing and undercrossing from (29) we have

$$\begin{aligned} & TrF^{-1}W(z_3, w)W(w, z_2)W(z_1, w)W(w, z_4)F^{-1} \\ & - (q^{\frac{1}{2}} - q^{-\frac{1}{2}})TrW(z_1, z_2)W(z_3, z_4) \\ & - Tr\langle FW(z_1, w)W(w, z_4)W(z_3, w)W(w, z_2)F \rangle = 0 \end{aligned} \quad (32)$$

Let us make a further twist that replace F^2 by F^2x where x denotes a nonzero variable. Then from (32) we have the following skein relation for the HOMFLY polynomial:

$$xL_+ + yL_0 - x^{-1}L_- = 0 \quad (33)$$

where we define $y = q^{-\frac{1}{2}} - q^{\frac{1}{2}}$ and that L_+ , L_0 and L_- are defined by

$$\begin{aligned} L_+ &= TrF^{-2}x^{-1}W(z_3, w)W(w, z_2)W(z_1, w)W(w, z_4) \\ L_0 &= TrW(z_1, z_2)W(z_3, z_4) \\ L_- &= TrxF^2W(z_1, w)W(w, z_4)W(z_3, w)W(w, z_2) \end{aligned} \quad (34)$$

which are as the HOMFLY polynomials for upcrossing, zero crossing and undercrossing respectively.

8 Defining quantum knots and knot invariant

Now we have that the quantum Wilson loop $W(z_1, z_1)$ corresponds to a closed curve in the complex plane with starting and ending point z_1 . Let this quantum Wilson loop $W(z_1, z_1)$ represents the unknot. We shall call $W(z_1, z_1)$ as the quantum unknot. Then from (19) we have the following invariant for the unknot:

$$TrW(z_1, z_1) = TrR^n A \quad n = 0, \pm 1, \pm 2, \dots \quad (35)$$

where $A = A_{14}$ is a 2-tensor constant matrix operator.

In the following let us extend the definition (35) to a knot invariant for nontrivial knots.

Let $W(z_i, z_j)$ represent a piece of curve with starting point z_i and ending point z_j . Then we let

$$W(z_1, z_2)W(z_3, z_4) \quad (36)$$

represent two pieces of uncrossing curve. Then by interchanging z_1 and z_3 we have

$$W(z_3, w)W(w, z_2)W(z_1, w)W(w, z_4) \quad (37)$$

represent the curve specified by $W(z_1, z_2)$ upcrossing the curve specified by $W(z_3, z_4)$.

Now for a given knot diagram we may cut it into a sum of parts which are formed by two pieces of curves crossing each other. Each of these parts is represented by (37) (For a knot diagram of the unknot with zero crossings we simply do not need to cut the knot diagram). Then we define the trace of a knot with a given knot diagram by the following form:

$$Tr \cdots W(z_3, w)W(w, z_2)W(z_1, w)W(w, z_4) \cdots \quad (38)$$

where we use (37) to represent the state of the two pieces of curves specified by $W(z_1, z_2)$ and $W(z_3, z_4)$. The \cdots means the product of a sequence of parts represented by (37) according to the state of each part. The ordering of the sequence in (38) follows the ordering of the parts given by the orientation of the knot diagram. We shall call the sequence of crossings in the trace (38) as the generalized Wilson loop of the knot diagram. For the knot diagram of the unknot with zero crossings we simply let it be $W(z, z)$ and call it the quantum Wilson loop.

We shall show that the generalized Wilson loop of a knot diagram has all the properties of the knot diagram and that (38) is a knot invariant. From this we shall call a generalized Wilson loop as a quantum knot.

9 Examples of quantum knots

Before the proof that a generalized Wilson loop of a knot diagram has all the properties of the knot diagram in the following let us first consider some examples to illustrate the way to define (38) and the way of applying the braiding formulas (24), (25) and (26) to equivalently transform (38) to a simple expression of the form $Tr R^{-m}W(z, z)$ where m is an integer.

Let us first consider the knot in Fig.1. For this knot we have that (38) is given by

$$Tr W(z_2, w)W(w, z_2)W(z_1, w)W(w, z_1) \quad (39)$$

where the product of quantum Wilson lines is from the definition (37) represented a crossing at w . In applying (37) we let z_1 be the starting and the ending point.



Fig.1

Then we have that (39) is equal to

$$\begin{aligned} & Tr W(w, z_2)W(z_1, w)W(w, z_1)W(z_2, w) \\ &= Tr RW(z_1, w)W(w, z_2)R^{-1}RW(z_2, w)W(w, z_1)R^{-1} \\ &= Tr W(z_1, z_2)W(z_2, z_1) \\ &= Tr W(z_1, z_1) \end{aligned} \quad (40)$$

where we have used (26). We see that (40) is just the knot invariant (35) of the unknot. Thus the knot in Fig.1 is with the same knot invariant of the unknot and this agrees with the fact that this knot is topologically equivalent to the unknot.

Then let us derive the Reidemeister move 1. Consider the diagram in Fig.2. We have that by (37) the definition (38) for this diagram is given by:

$$\begin{aligned} & Tr \langle W(z_2, w)W(w, z_2)W(z_1, w)W(w, z_3) \rangle \\ &= Tr \langle W(z_2, w)RW(z_1, w)W(w, z_2)R^{-1}W(w, z_3) \rangle \\ &= Tr \langle W(z_2, w)RW(z_1, z_2)R^{-1}W(w, z_3) \rangle \\ &= Tr \langle R^{-1}W(w, z_3)W(z_2, w)RW(z_1, z_2) \rangle \\ &= Tr \langle W(z_2, w)W(w, z_3)W(z_1, z_2) \rangle \\ &= Tr \langle W(z_2, z_3)W(z_1, z_2) \rangle \\ &= Tr \langle W(z_1, z_3) \rangle \end{aligned} \quad (41)$$

where $W(z_1, z_3)$ represent a piece of curve with initial end point z_1 and final end point z_3 which has no crossing. When Fig.2 is a part of a knot we can also derive a result similar to (41) which is for the Reidemeister move 1. This shows that the Reidemeister move 1 holds. Then let us derive Reidemeister

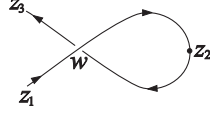


Fig.2

move 2. By (37) we have that the definition (38) for the two pieces of curve in Fig.3a is given by

$$\begin{aligned} & Tr\langle W(z_5, w_1)W(w_1, z_2)W(z_1, w_1)W(w_1, z_6) \cdot \\ & W(z_4, w_2)W(w_2, z_3)W(z_2, w_2)W(w_2, z_5) \rangle \end{aligned} \quad (42)$$

where the two products of W separated by the \cdot are for the two crossings in Fig.3a. We have that (42) is equal to

$$\begin{aligned} & Tr\langle W(z_4, w_2)W(w_2, z_3)W(z_2, w_2)W(w_2, z_5) \cdot \\ & W(z_5, w_1)W(w_1, z_2)W(z_1, w_1)W(w_1, z_6) \rangle \\ = & Tr\langle W(z_1, z_3)W(z_4, z_6) \rangle \end{aligned} \quad (43)$$

where we have repeatedly used (26). This shows that the diagram in Fig.3a is equivalent to two uncrossing curves. When Fig.3a is a part of a knot we can also derive a result similar to (43) for the Reidemeister move 2. This shows that the Reidemeister move 2 holds. As an illustration let us consider the knot in

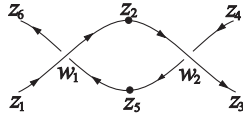


Fig.3a

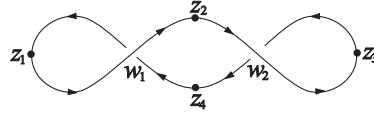


Fig.3b

Fig.3b which is related to the Reidemeister move 2. By (37) we have that the definition (38) for this knot is given by

$$\begin{aligned} & Tr\langle W(z_3, w_2)W(w_2, z_3)W(z_2, w_2)W(w_2, z_4) \cdot \\ & W(z_4, w_1)W(w_1, z_2)W(z_1, w_1)W(w_1, z_1) \rangle \\ = & Tr\langle RW(z_2, w_2)W(w_2, z_3)W(z_3, w_2)W(w_2, z_4) \cdot \\ & W(z_4, w_1)W(w_1, z_1)W(z_1, w_1)W(w_1, z_2)R^{-1} \rangle \\ = & Tr\langle W(z_2, w_2)W(w_2, z_3)W(z_3, w_2)W(w_2, z_4) \cdot \\ & W(z_4, w_1)W(w_1, z_1)W(z_1, w_1)W(w_1, z_2) \rangle \\ = & Tr\langle W(z_2, z_2) \rangle \end{aligned} \quad (44)$$

where we let the curve be with z_2 as the initial and final end point and we have used (24) and (25). This shows that the knot in Fig.3b is with the same knot invariant of a trivial knot. This agrees with the fact that this knot is equivalent to the trivial knot. Similar to the above derivations we can derive the Reidemeister move 3.

Let us then consider a trefoil knot in Fig.4a. By (37) and similar to the above examples we have that the definition (38) for this knot is given by:

$$\begin{aligned} & Tr\langle W(z_4, w_1)W(w_1, z_2)W(z_1, w_1)W(w_1, z_5) \cdot W(z_2, w_2)W(w_2, z_6) \\ & W(z_5, w_2)W(w_2, z_3) \cdot W(z_6, w_3)W(w_3, z_4)W(z_3, w_3)W(w_3, z_1) \rangle \\ = & Tr\langle W(z_6, z_1)W(z_3, z_6)W(z_1, z_3) \rangle \end{aligned} \quad (45)$$

where we have repeatedly used (26). Then we have that (45) is equal to:

$$\begin{aligned}
& Tr\langle W(z_6, w_3)W(w_3, z_1)W(z_3, w_3)W(w_3, z_6)W(z_1, z_3)\rangle \\
&= Tr\langle RW(z_3, w_3)W(w_3, z_1)W(z_6, w_3)W(w_3, z_6)W(z_1, z_3)\rangle \\
&= Tr\langle RW(z_3, w_3)RW(z_6, w_3)W(w_3, z_1)R^{-1}W(w_3, z_6)W(z_1, z_3)\rangle \\
&= Tr\langle W(z_3, w_3)RW(z_6, z_1)R^{-1}W(w_3, z_6)W(z_1, z_3)R\rangle \\
&= Tr\langle W(z_3, w_3)RW(z_6, z_3)W(w_3, z_6)\rangle \\
&= Tr\langle W(w_3, z_6)W(z_3, w_3)RW(z_6, z_3)\rangle \\
&= Tr\langle RW(z_3, w_3)W(w_3, z_6)W(z_6, z_3)\rangle \\
&= Tr\langle RW(z_3, z_3)\rangle
\end{aligned} \tag{46}$$

where we have used (24) and (26). We see that (46) is a knot invariant for the trefoil knot in Fig.4a. Similarly for the trefoil knot in Fig. 4b which is the mirror image of the trefoil knot in Fig.4a we have

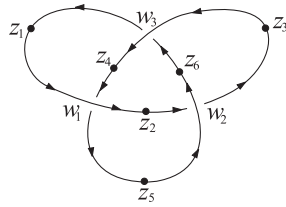


Fig.4a

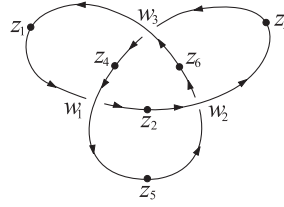


Fig.4b

that the definition (38) for this knot is equal to $Tr\langle W(z_5, z_5)R^{-1}\rangle$ which is a knot invariant for the trefoil knot in Fig.4b. We notice that this knot invariant is different from (46). This shows that these two trefoil knots are not topologically equivalent.

With the above new knot invariants we can now give a classification of knots. Let C_1 and C_2 be two knots. Then since we can derive the Reidemeister moves by using (24), (25) and (26), we have that C_1 and C_2 are topologically equivalent if and only if the W -product and the correlation (38) for C_1 can be transformed to the W -product and the correlation (38) for C_2 by using (24), (25) and (26). Thus correlations (38) are knot invariants which can completely classify knots. In [15], we use other approach to show that knots can be classified by the number of product of R and R^{-1} matrices. More calculations and examples of the above knot invariants will be given elsewhere.

10 Quantum knots as gluons and quantum Wilson line as gloun propagator

Since the quantum knot based on the $U(1)$ group has properties of photon with winding numbers as frequencies and with the loop nature giving the spin, it is as the model of photon. Then we let quantum knots based on $SU(2)$ and $SU(3)$ be as models of gluons.

When the quantum knots act on complex vectors representing spinors (for electrons or quarks), the quantum knots together with the complex vectors are as models of electron, mesons and baryons. For example, the meson π is modeled by quantum prime knot $\mathbf{4}_1$, and the proton is modeled by the quantum prime knot $\mathbf{6}_2$. More details of modeling elementary particles by quantum knots are given in [15].

Let us then investigate the quantum Wilson line $W(z_0, z)$ with $SU(2) \otimes U(1)$ (or $SU(3) \otimes U(1)$) group where z_0 is fixed for the gloun field. We want to show that this quantum Wilson line $W(z_0, z)$ may be regarded as the quantum gloun propagator for a gloun propagating from z_0 to z . This quantum gloun propagator will give the nuclear forces for the scattering interaction of nucleons such as proton p and neutron n . When the gauge group is the $U(1)$ group, the quantum Wilson line $W(z_0, z)$ is regarded as the quantum photon propagator for a photon propagating from z_0 to z .

Let us first consider the $U(1)$ gauge group. As we have shown in the above section on computation of quantum Wilson line; to compute $W(z_0, z)$ we need to write $W(z_0, z)$ in the form of two (connected)

Wilson lines: $W(z_0, z) = W(z_0, z_1)W(z_1, z)$ for some z_1 point. Then we have:

$$W(z_0, z_1)W(z_1, z) = e^{-\hat{t} \log[\pm(z_1 - z_0)]} A e^{\hat{t} \log[\pm(z - z_1)]} \quad (47)$$

where $\hat{t} = -\frac{e_0^2}{k_0}$ for the $U(1)$ group ($k_0 > 0$ is a constant and we may for simplicity let $k_0 = 1$) where the term $e^{-\hat{t} \log[\pm(z_1 - z_0)]}$ is obtained by solving the first form of the dual form of the KZ equation and the term $e^{\hat{t} \log[\pm(z - z_1)]}$ is obtained by solving the second form of the dual form of the KZ equation.

Then we may write $W(z_0, z)$ in the following form:

$$W(z_0, z) = W(z_0, z_1)W(z_1, z) = e^{-\hat{t} \log \frac{(z_1 - z_0)}{(z - z_1)}} A \quad (48)$$

Let us fix z_1 with z such that:

$$\frac{|z_1 - z_0|}{|z - z_1|} = \frac{r_1}{n_e^2} \quad (49)$$

for some positive integer n_e such that $r_1 \geq n_e^2$; and we let z be a point on a path of connecting z_0 and z_1 and then a closed loop is formed with z as the starting and ending point. (This loop can just be the photon-loop of the electron in this electromagnetic interaction by this photon propagator (48).) Then (48) has a factor $e_0^2 \log \frac{r_1}{n_e^2}$ which is the fundamental solution of the two dimensional Laplace equation and is analogous to the fundamental solution $-\frac{e^2}{r}$ (where $e := e_0 n_e$ denotes the observed (renormalized) electric charge and r denotes the three dimensional distance) of the three dimensional Laplace equation for the Coulomb's law. Thus the operator $W(z_0, z) = W(z_0, z_1)W(z_1, z)$ in (48) can be regarded as the quantum photon propagator propagating from z_0 to z .

We remark that when there are many photons we may introduce the space variable x via the Lorentz metric $ds^2 = dt^2 - dx^2$ as a statistical variable to obtain the Coulomb's law $\frac{e^2}{r}$ from the fundamental solution $e_0^2 \log \frac{r_1}{n_e^2}$ as a statistical law for electricity.

The quantum photon propagator (48) gives a repulsive effect since it is analogous to the Coulomb's law $-\frac{e^2}{r}$. On the other hand we can reverse the sign of \hat{t} such that this photon operator can also give an attractive effect:

$$W(z_0, z) = W(z_0, z_1)W(z_1, z) = e^{\hat{t} \log \frac{(z - z_1)}{(z_1 - z_0)}} A, \quad (50)$$

where we fix z_1 with z_0 such that:

$$\frac{|z - z_1|}{|z_1 - z_0|} = \frac{r_1}{n_e^2} \quad (51)$$

for some positive integer n_e such that $r_1 \geq n_e^2$; and we again let z be a point on a path of connecting z_0 and z_1 and then a closed loop is formed with z as the starting and ending point. (This loop again can just be the photon-loop of the electron in this electromagnetic interaction by this photon propagator (48).)

Thus the quantum photon propagator in (48) (and in (50)) can give repulsive or attractive effect between two points z_0 and z for all z in the complex plane. These repulsive or attractive effects of the quantum photon propagator correspond to two charges of the same sign and of different sign respectively.

Let us then derive a classical photon propagator from the quantum photon propagator $W(z_0, z)$. Let us choose a path connecting z_0 and z . Let us consider the following path:

$$z = z(s) = z_1 + a_0[\theta(s_1 - s)e^{-i\beta_1(s_1 - s)} + \theta(s - s_1)e^{i\beta_1(s_1 - s)}] \quad (52)$$

where $\beta_1 > 0$ is a parameter and $z(s_0) = z_0$ for some proper time s_0 ; and a_0 is some complex constant; and θ is a step function given by $\theta(s) = 0$ for $s < 0$, $\theta(s) = 1$ for $s \geq 0$. Then on this path we have:

$$\begin{aligned} W(z_0, z) &= W(z_0, z_1)W(z_1, z) = e^{\hat{t} \log \frac{(z - z_1)}{(z_1 - z_0)}} A = e^{\hat{t} \log \frac{a_0[\theta(s - s_1)e^{-i\beta_1(s_1 - s)} + \theta(s_1 - s)e^{i\beta_1(s_1 - s)}]}{(z_1 - z_0)}} A \\ &= e^{\hat{t} \log b[\theta(s - s_1)e^{-i\beta_1(s_1 - s)} + \theta(s_1 - s)e^{i\beta_1(s_1 - s)}]} A = b_0[\theta(s - s_1)e^{-i\hat{t}\beta_1(s_1 - s)} + \theta(s_1 - s)e^{i\hat{t}\beta_1(s_1 - s)}] A \end{aligned} \quad (53)$$

for some complex constants b and b_0 . From this chosen of the path (52) we have that the quantum photon propagator is proportional to the following expression:

$$\frac{1}{2\lambda_1}[\theta(s-s_1)e^{-i\lambda_1(s-s_1)} + \theta(s_1-s)e^{i\lambda_1(s-s_1)}] \quad (54)$$

where we define $\lambda_1 = -\hat{t}\beta_1 = e_0^2\beta_1 > 0$. We see that this is the usual propagator of a particle $x(s)$ of harmonic oscillator with mass-energy parameter $\lambda_1 > 0$ where $x(s)$ satisfies the following harmonic oscillator equation:

$$\frac{d^2x}{ds^2} = -\lambda_1^2 x(s) \quad (55)$$

We regard (54) as the propagator of a photon with mass-energy parameter λ_1 . Fourier transforming (54) we have the following form of photon propagator:

$$\frac{i}{k_E^2 - \lambda_1^2} \quad (56)$$

Then when the gauge group is the $SU(2) \otimes U(1)$ (or $SU(3) \otimes U(1)$) group the analysis is similar to the case of $U(1)$ group. In the following section we show that the corresponding quantum gluon propagator gives the nuclear force.

11 Quantum gluon propagator as nuclear potential

Let the quantum Wilson line $W(z_0, z_1)W(z_1, z)$ be as a quantum gluon propagator. Let

$$\mathbf{p}_i := W(K_i)Z_i \quad (57)$$

$i = 1, 2$ denotes two protons. Then the quantum gluon propagator $W(z_0, z_1)W(z_1, z)$ represents a nuclear force on the interaction of $\mathbf{p}_i, i = 1, 2$ by the following formula:

$$\mathbf{p}_1^* W(z_0, z_1) W(z_1, z) \mathbf{p}_2 \quad (58)$$

Similarly let

$$\mathbf{n}_i := W(K_i)Z_i \quad (59)$$

$i = 1, 2$ denotes two neutrons. Then the quantum gluon propagator $W(z_0, z_1)W(z_1, z)$ represents a nuclear force on the interaction of $\mathbf{n}_i, i = 1, 2$ by the following formula:

$$\mathbf{n}_1^* W(z_0, z_1) W(z_1, z) \mathbf{n}_2 \quad (60)$$

Then the quantum gluon propagator $W(z_0, z_1)W(z_1, z)$ represents a nuclear force on the interaction of \mathbf{p} and \mathbf{n} by the following formula:

$$\mathbf{n}^* W(z_0, z_1) W(z_1, z) \mathbf{p} \quad (61)$$

For the quantum gluon propagator, for simplicity we consider the $SU(2) \otimes U(1)$ group which is as a subgroup of $SU(3) \otimes U(1)$. We have:

$$\hat{t} := \frac{e_0^2}{k_0 + g_0} \sum_a t^a \otimes t^a \quad (62)$$

where $t^a = iT^a$ and:

$$T^1 = \begin{pmatrix} 0 & 1 \\ 1 & 0 \end{pmatrix}, \quad T^2 = \begin{pmatrix} 0 & i \\ -i & 0 \end{pmatrix}, \quad T^3 = \begin{pmatrix} 1 & 0 \\ 0 & -1 \end{pmatrix} \quad (63)$$

Let us call this Casimir operator T as the mass operator for the π mesons. We have

$$T = \sum_{a=1}^3 T^a \otimes T^a = \begin{pmatrix} 1 & 0 & 0 & 0 \\ 0 & -1 & 2 & 0 \\ 0 & 2 & -1 & 0 \\ 0 & 0 & 0 & 1 \end{pmatrix} \quad (64)$$

This Casimir operator has eigenvalues 1 and -3 where 1 is with multiplicity 3. Since 1 is positive it is considered as an eigenvalue for mass and energy. The negative eigenvalue -3 is considered to be nonphysical. It can be checked that

$$v_1 = \begin{pmatrix} 1 \\ 0 \\ 0 \\ 0 \end{pmatrix}, \quad v_3 = \begin{pmatrix} 0 \\ \frac{1}{2} \\ \frac{1}{2} \\ 0 \end{pmatrix}, \quad v_4 = \begin{pmatrix} 0 \\ 0 \\ 0 \\ 1 \end{pmatrix}, \quad (65)$$

are three independent eigenvectors for the eigenvalue 1. We show in [15] that the eigenvalue 1 gives the mass 135MeV for the π^0 meson.

Then an eigenvector of -3 is given by:

$$v_2 = \begin{pmatrix} 0 \\ \frac{1}{2} \\ \frac{1}{2} \\ 0 \end{pmatrix} \quad (66)$$

We can write T in the diagonalized form:

$$T = \begin{pmatrix} v_1 & v_2 & v_3 & v_4 \end{pmatrix} \begin{pmatrix} 1 & 0 & 0 & 0 \\ 0 & -3 & 0 & 0 \\ 0 & 0 & 1 & 0 \\ 0 & 0 & 0 & 1 \end{pmatrix} \begin{pmatrix} v_1 & v_2 & v_3 & v_4 \end{pmatrix}^{-1} =: VDV^{-1} \quad (67)$$

As the photon case, the eigenvalue 1 for $r_1 > n_e^2$ gives repulsive effect for the interacting elementary particles such as \mathbf{p} and \mathbf{n} . This gives the effect of the π^0 meson for the nuclear force induced by the π^0 meson. Thus the quantum gluon propagator includes the repulsive effect of the scattering of nucleons such as \mathbf{p} , \mathbf{n} by the exchange of the π^0 meson.

Then eigenvalue -3 for $r_1 > n_e^2$ gives attractive effect for the interacting elementary particles such as \mathbf{p} and \mathbf{n} . Thus the quantum gluon propagator includes the attractive and repulsive effect of the scattering of nucleons such as \mathbf{p} , \mathbf{n} . Statistically, when $r_1 > n_e^2$ and $r_1 - n_e^2$ is small, the attractive and repulsive effects are respectively given by:

$$\frac{3e^2}{r} \quad \text{and} \quad \frac{-e^2}{r} \quad (68)$$

where r is the usual three dimensional space distance. Then since $|-3| > 1$ we have that the attractive effect by -3 is greater than the repulsive effect by 1. Thus the nuclear interaction of nucleon such as \mathbf{p} , \mathbf{n} is attractive in the forming of nuclei since this is the case of $r_1 > n_e^2$ and $r_1 - n_e^2$ is small.

Then we notice that when $r_1 < n_e^2$ we have that the interacting potential of the quantum gluon propagator of the eigenvalue -3 gives repulsive effect which is greater than the attractive effect of the eigenvalue 1. Thus when the distance between the nucleons is very small (or $r_1 < n_e^2$) we have that the force between the nucleons is repulsive. This agrees with the experiments that the nuclear force between the nucleons is repulsive when the distance between the nucleons is very small.

On the other hand when r_1 is large such that $r_1 \gg n_e^2$ we have that the effect of quantum gluon propagator of the eigenvalue -3 is much smaller than the effect of quantum gluon propagator of the eigenvalue 1 since we have:

$$e^{-3 \log \frac{r_1}{n_e^2}} \rightarrow 0 \quad \text{as} \quad r_1 \rightarrow \infty. \quad (69)$$

Thus the net effect of the quantum gloun propagator is repulsive when r_1 is large. This agrees with the experiments of the neuclear force.

Then because of the mass term of the quantum gloun propagator is larger than that of the quantum photon propagator we have that the repulsive effect of the quantum gloun propagator is of short range while the repulsive effect of the electromagnetic interaction is of long range. Thus the quantum gloun propagator gives the nuclear force for the scattering interaction of nucleons and for the forming of nuclei.

The quantum gloun propagator gives the nuclear force for the scattering interaction of nucleons and for the forming of nuclei. Thus this quantum gloun propagator can be used to replace the Paris potential for the scattering interection of nucleons.

Let us consider the knot model of an elementary particle such as the following knot model of proton:

$$\mathbf{p} = W(K)Z(s) \quad (70)$$

where the quark components of $Z(s)$ are at proper time s forming the vector $Z(s)$. In this case the quantum knot $W(K)$ is a gloun propagator in closed form with $z_0 = z$. Because of the closed form we have that the net interaction effect from the gloun propagator is zero. Thus the net interaction effect of the quark components of $Z(s)$ is zero. Thus this knot model of proton gives the asymptotic freedom property of strong interaction of the quarks of the proton \mathbf{p} .

Let us then derive (and define) a classical gloun propagator from the quantum gloun propagator. As the photon case let us choose a path connecting z_0 and z . Let us consider the path (52). From this chosen of the path (52) we have that the quantum gloun propagator is proportional to the following expression:

$$V \frac{1}{2\lambda_1} [\theta(s - s_1)e^{-iD_1(s-s_1)} + \theta(s_1 - s)e^{iD_1(s-s_1)}] V^{-1} \quad (71)$$

where we define $D_1 = -De_0^2\beta_1$.

12 Renormalization group method for critical phenomena of QED

In this section and the following sections we shall show that the QED model (1) with the parameter $\frac{1}{i\hbar+\kappa}$ is a model of superconductivity and magnetism. We shall continue to show that the Planck constant parameter $\hbar \neq 0$ basically gives dynamical wave effects and conductivity while the parameter $\kappa > 0$ basically gives magnetic effects. For this QED model (1) to be a model of superconductivity and magnetism we introduce many variables Z_a for electrons indexed by a and many variables A_{1b}, A_{2b} for photons indexed by b which are coupled together with the following seagull vertex:

$$- \frac{1}{i\hbar + \kappa} e^2 Z_a^* Z_a A_b^2 \quad (72)$$

and the usual vertex for QED (giving the Coulomb potential) in (1) with a single $\frac{dZ_a}{ds}$. We shall show that the coupling term (72) gives critical phenomena which gives the phenomena of superconductivity and magnetism.

From the interaction term (72) the one-loop mass-energy term of electron and photon are respectively given by:

$$\frac{e^2}{(i\hbar+\kappa)} \frac{1}{2\pi} \int \frac{dk}{\frac{1}{(i\hbar+\kappa)^2} k^2 + \lambda_1^2} = \frac{e^2}{(i\hbar+\kappa)} \frac{(i\hbar+\kappa)}{2\pi} \int \frac{dk}{k^2 + (i\hbar+\kappa)^2 \lambda_1^2} = \frac{e^2}{2(i\hbar+\kappa)\lambda_1} =: \frac{\omega^2}{(i\hbar+\kappa)} =: \omega^2(-i\bar{\hbar} + \bar{\kappa}) =: r \quad (73)$$

and

$$\frac{e^2}{(i\hbar+\kappa)} \frac{1}{2\pi} \int \frac{dq}{\frac{1}{(i\hbar+\kappa)^2} q^2 + \mu^2} = \frac{e^2}{(i\hbar+\kappa)} \frac{(i\hbar+\kappa)}{2\pi} \int \frac{dq}{q^2 + (i\hbar+\kappa)^2 \mu^2} = \frac{e^2}{2(i\hbar+\kappa)\mu} =: \frac{\lambda_2^2}{(i\hbar+\kappa)} =: -i\bar{\lambda}_2^2 \bar{\hbar} + \bar{\lambda}_2^2 \bar{\kappa} \quad (74)$$

In terms of Feymann diagram the above formula (73) shows that a photon line in the forming of a closed loop gives a photon propagator of the form $\frac{i\hbar+\kappa}{k^2+(i\hbar+\kappa)^2\lambda_1^2}$. Also the above formula (74) shows that an

electron line in the forming of a closed loop gives an electron propagator of the form $\frac{ih+\kappa}{q^2+(ih+\kappa)^2\mu^2}$. In these two formulae each e^2 gives a factor $\frac{1}{ih+\kappa}$.

Similarly for the two-loop case (with one photon loop and one electron loop where the photon loop consists of two photon lines and the electron loop consists of one electron line) constructed by (72) the mass-energy term of electron is given by:

$$-\frac{e^4}{(ih+\kappa)^2} \frac{(ih+\kappa)^3}{(2\pi)^2} \int \frac{dkdq}{(k^2+(ih+\kappa)^2\lambda_1^2)(q^2+(ih+\kappa)^2\mu^2)} = -\frac{e^4}{8(ih+\kappa)^3\lambda_1^3\mu} = -\frac{e^4((\bar{\kappa}^2-\bar{h}^2)-2i\bar{\kappa}\bar{h})(-i\bar{h}+\bar{\kappa})}{8\lambda_1^3\mu} \quad (75)$$

where the factor $(ih+\kappa)^3$ is from the two photon lines and one electron line.

Then for the three-loop case (with two photon loops and one electron loop where one photon loop consists of two photon lines and the electron loop consists of two electron lines while the other photon loop consists of one photon line, as the case of (73)) constructed by (72) we have that the mass-energy term is given by:

$$\begin{aligned} & \frac{e^6}{(ih+\kappa)^3} \frac{(ih+\kappa)^5}{(2\pi)^3} \int \frac{dkdqdl}{(k^2+(ih+\kappa)^2\lambda_1^2)(q^2+(ih+\kappa)^2\mu^2)(l^2+(ih+\kappa)^2\lambda_1^2)} \\ &= \frac{e^6}{32(ih+\kappa)^5\lambda_1^4\mu^3} = \frac{e^6[(\bar{\kappa}^3-3\bar{\kappa}\bar{h}^2)-i(3\bar{\kappa}^2\bar{h}-\bar{h}^3)](-ih+\kappa)^2}{32\lambda_1^4\mu^3} \end{aligned} \quad (76)$$

where the factor $(ih+\kappa)^5$ is from the the three photon lines and the two electron lines.

Then we consider the four point vertex with four external electron lines. From (72) the one-photon-loop interaction term is given by:

$$I_1(p_1+p_2) = \frac{e^4(ih+\kappa)^2}{(ih+\kappa)^2(2\pi)} \int \frac{dk}{(k^2+(ih+\kappa)^2\lambda_2^2)((p_1+p_2-k)^2+(ih+\kappa)^2\lambda_2^2)} \quad (77)$$

where p_1, p_2 are the momentums of two external electron lines respectively, and the two photon propagators are obtained by the Dyson geometry series.

Setting $p_1, p_2 = 0$ we get an interaction constant u given by

$$u := 2I_1(0) = \frac{e^4}{2(ih+\kappa)^3\lambda_2^3} = \frac{e^4[(\bar{\kappa}^3-3\bar{h}^2)-i(3\bar{\kappa}^2\bar{h}-\bar{h}^3)]}{2\lambda_2^3} \quad (78)$$

where the coefficient 2 comes from permutation of $I_1(p_1+p_2)$.

Similarly from (72) the three-loop interaction term (two photon-loops and one electron-loop) of the four point vertex is given by

$$\begin{aligned} I_2(p_1+p_2) &= \frac{e^8(ih+\kappa)^6}{(ih+\kappa)^4(2\pi)^3} \int \frac{dkdqdl}{(k^2+(ih+\kappa)^2\lambda_2^2)((p_1+p_2-k)^2+(ih+\kappa)^2\lambda_2^2)(q^2+(ih+\kappa)^2\omega^2)} \times \\ &\times \frac{1}{((p_1+p_2-q)^2+(ih+\kappa)^2\omega^2)((p_1+p_2-l)^2+(ih+\kappa)^2\lambda_2^2)} \frac{1}{(l^2+(ih+\kappa)^2\lambda_2^2)((p_1+p_2-l)^2+(ih+\kappa)^2\lambda_2^2)} \end{aligned} \quad (79)$$

where the photon propagators and electron propagators are obtained by the Dyson geometry series. Setting $p_1, p_2 = 0$ we have the following interaction constant which will be added to (78):

$$2I_2(0) = \frac{e^8}{32(ih+\kappa)^7\lambda_2^6\omega^3} \quad (80)$$

By re-scaling λ_1, μ to λ'_1, μ' from (73)-(80) we re-scale r to r' and u to u' given by

$$\begin{aligned} r' &= \frac{e^2}{2(ih+\kappa)\lambda'_1} - \frac{e^4}{8(ih+\kappa)^3\lambda_1^3\mu'} + \frac{e^6}{32(ih+\kappa)^5\lambda_1^4\mu'^3} \\ u' &= \frac{e^4}{2(ih+\kappa)^3\lambda_2^3} + \frac{e^8}{32(ih+\kappa)^7\lambda_2^6\omega'^3} \end{aligned} \quad (81)$$

From (81) we get the following renormalization-group recursion equation:

$$\begin{aligned} r' &= b^2r - Ab^{6-\frac{2}{3}\epsilon}r^3u^{-\frac{2}{3}} + Cb^{8-2\epsilon}r^4u^{-2} \\ u' &= b^\epsilon u + Bb^{2\epsilon-3}u^2r^{-\frac{3}{2}} \end{aligned} \quad (82)$$

where we define

$$\frac{\lambda_1}{\lambda'_1} = b^2 \quad \text{and} \quad \frac{\mu'}{\mu} = b^{\frac{2}{3}\epsilon} \quad (83)$$

where b is regarded as a scale factor and $\epsilon > 0$ is a parameter which is analogous to the ϵ in the ϵ -expansion of the Ginzburg-Landau-Wilson (GLW) model in statistical physics [16]-[20]; and

$$A = \frac{2^{\frac{1}{3}}}{e^{\frac{4}{3}}(ih + \kappa)^2}, \quad B = \frac{1}{8(ih + \kappa)^{\frac{5}{2}}}, \quad C = \frac{1}{(ih + \kappa)^7} \quad (84)$$

As analogous to the GLW model the parameter ϵ is related to the dimension of the space [16]-[20]. Thus as a space-time statistics we consider that ϵ is related to the space-time statistics that $d = 3 - \epsilon$ is the (fractional) dimension of the space, which is related to the ultraviolet limit, as we have considered in the above sections; while the parameter b is related to the infrared limit.

We remark that (82) is analogous to the renormalization-group equation of the Ginzburg-Landau-Wilson model in statistical physics. We may regard the GLW model as an approximation of this QED statistical model.

Following the renormalization group method in statistical physics we set up the following equation to find fixed points of (82):

$$\begin{aligned} r &= b^2 r - Ab^{6-\frac{2}{3}\epsilon} r^3 u^{-\frac{2}{3}} + Cb^{8-2\epsilon} r^4 u^{-2} \\ u &= b^\epsilon u + Bb^{2\epsilon-3} u^2 r^{-\frac{3}{2}} \end{aligned} \quad (85)$$

The nontrivial fixed point is given by:

$$\begin{aligned} r^* &= B^{-\frac{2}{3}} \frac{(1-b^\epsilon)^{\frac{2}{3}} [b^2 - 1 + \frac{CB^2 b^{2+2\epsilon}}{(1-b^\epsilon)^2}]}{Ab^{4+\frac{2}{3}\epsilon}} \\ u^* &= B^{-2} \frac{(1-b^\epsilon)^2 [b^2 - 1 + \frac{CB^2 b^{2+2\epsilon}}{(1-b^\epsilon)^2}]^{\frac{3}{2}}}{A^{\frac{3}{2}} b^{3+3\epsilon}} \end{aligned} \quad (86)$$

Linearizing the renormalization-group transformation near the fixed point (86) we get the linearized transformation matrix. We consider two cases:

Case 1). $\epsilon \ll 1$ and b is large such that $\epsilon \log b$ is very small;

Case 2). $\epsilon = 1$, and $b < 1$, $b \rightarrow 1$ such that $\epsilon |\log b| = |\log b|$ is very small.

For these two cases the eigenvalues of this matrix are approximately given by:

$$\begin{aligned} \lambda_{R1} &\approx b^2 [-2 + CB^2 b^{2\epsilon} (b^\epsilon - 1)^{-2}] \\ &\approx b^2 [-2 + CB^2 (3 - 2\epsilon \ln b)] \end{aligned} \quad (87)$$

$$\lambda_{R2} \approx 0$$

Let us first consider the Case 1). From (87) a rough estimate for $\lambda_{R1} > 1$ is:

$$-2 + \text{Re}CB^2 > 0 \quad (88)$$

and

$$\text{Im}CB^2 = 0 \quad (89)$$

From (87) we have that when (88) and (89) hold the critical exponent ν of correlation length is given by:

$$\begin{aligned} \nu &= \frac{\ln b}{\ln \lambda_{R1}} \approx \frac{1}{2} + \frac{2\text{Re}CB^2 \epsilon}{2(-2+3\text{Re}CB^2)} \\ &= \frac{1}{2} + \frac{\epsilon}{2} \end{aligned} \quad (90)$$

Thus for this Case 1) (which means that the dimension of the space is 3) we have that $\frac{1}{2} < \nu < 1$.

Let us then consider the Case 2). For this case the dimension of space is $3 - \epsilon = 2$. From (87) a rough estimate for $\lambda_{R1} > 1$ is:

$$\text{Re}CB^2 > 0 \quad (91)$$

and

$$\text{Im}CB^2 = 0 \quad (92)$$

From (87) we have that when (91) and (92) hold the critical exponent ν of correlation length is given by:

$$\begin{aligned} \nu &= \frac{\ln b}{\ln \lambda_{R1}} \approx \frac{1}{2} + \frac{2\text{Re}CB^2\epsilon}{4\text{Re}CB^2} \\ &= \frac{1}{2} + \frac{\epsilon}{2} = 1 \end{aligned} \quad (93)$$

Thus for this Case 2) (which means that the dimension of the space is 2) we have that $\nu = 1$. It is interesting that this is just the result given by the exact solution of the two dimensional Ising model [17, 20].

13 Renormalization group method for critical phenomena of QCD

In this section we consider the QCD model (3) with the parameter $\frac{1}{ih+\kappa}$. We shall continue to show that the Planck constant parameter $h \neq 0$ basically gives dynamical wave effects and conductivity while the parameter $\kappa > 0$ basically gives magnetic effects.

For this QCD model (3), as the QED model (1), we introduce many variables Z_a for quarks indexed by a and many variables A_{1b}, A_{2b} for gluon indexed by b which are coupled together with the following seagull vertex:

$$-\frac{1}{ih+\kappa}e^2Z_a^*Z_aA_b^2 \quad (94)$$

For the component of gluon propagator with respect to the eigenvalue 1, the result of the renormalization group method is exactly the same as the QED case. Let us then consider the component of gluon propagator with respect to the eigenvalue -3 . In this case the classical component of gluon propagator is given by:

$$\frac{i}{k_E^2 - 3^2\lambda_1^2} \quad (95)$$

when $h = 1, \kappa \rightarrow 0$.

Then, for general h, κ , as the QED case, we have the following renormalization group equation:

$$\begin{aligned} r' &= b^2r - \frac{1}{3^2}Ab^{6-\frac{2}{3}\epsilon}r^3u^{-\frac{2}{3}} + \frac{1}{3^3}Cb^{8-2\epsilon}r^4u^{-2} \\ u' &= b^\epsilon u + Bb^{2\epsilon-3}u^2r^{-\frac{3}{2}} \end{aligned} \quad (96)$$

where r is defined in (73) and the equation of r' is obtained by multiplying 3 to get the right hand side of the equation of r' .

Thus for the QCD case we have two renormalization group equations (96) and (82).

Then we set up the following equation to find fixed points of (96):

$$\begin{aligned} r &= b^2r - \frac{1}{3^2}Ab^{6-\frac{2}{3}\epsilon}r^3u^{-\frac{2}{3}} + \frac{1}{3^3}Cb^{8-2\epsilon}r^4u^{-2} \\ u &= b^\epsilon u + Bb^{2\epsilon-3}u^2r^{-\frac{3}{2}} \end{aligned} \quad (97)$$

The nontrivial fixed point is given by:

$$\begin{aligned} r^* &= B^{-\frac{2}{3}} \frac{(1-b^\epsilon)^{\frac{2}{3}} [b^2 - 1 + \frac{3^{-3}CB^2b^{2+2\epsilon}}{(1-b^\epsilon)^2}]}{3^{-2}Ab^{4+\frac{2}{3}\epsilon}} \\ u^* &= B^{-2} \frac{(1-b^\epsilon)^2 [b^2 - 1 + \frac{3^{-3}CB^2b^{2+2\epsilon}}{(1-b^\epsilon)^2}]^{\frac{3}{2}}}{3^{-3}A^{\frac{3}{2}}b^{3+3\epsilon}} \end{aligned} \quad (98)$$

Linearizing the renormalization-group transformation near the fixed point (98) we get the linearized transformation matrix. We consider two cases:

Case 1). $\epsilon \ll 1$ and b is large such that $\epsilon \log b$ is very small;

Case 2). $\epsilon = 1$, and $b < 1$, $b \rightarrow 1$ such that $\epsilon |\log b| = |\log b|$ is very small.

For these two cases the eigenvalues of this matrix are approximately given by:

$$\begin{aligned}\lambda_{R1} &\approx b^2[-2 + \frac{1}{3^3}CB^2b^{2\epsilon}(b^\epsilon - 1)^{-2}] \\ &\approx b^2[-2 + \frac{1}{3^3}CB^2(3 - 2\epsilon \ln b)] \\ \lambda_{R2} &\approx 0\end{aligned}\tag{99}$$

Let us first consider the Case 1). From (87) a rough estimate for $\lambda_{R1} > 1$ is:

$$-2 + \text{Re} \frac{1}{3^3}CB^2 > 0\tag{100}$$

and

$$\text{Im} \frac{1}{3^3}CB^2 = 0\tag{101}$$

Let us then consider the Case 2). For this case the dimension of space is $3 - \epsilon = 2$. From (87) a rough estimate for $\lambda_{R1} > 1$ is:

$$\text{Re} \frac{1}{3^3}CB^2 > 0\tag{102}$$

and

$$\text{Im} \frac{1}{3^3}CB^2 = 0\tag{103}$$

Thus for QCD case, we have two nontrivial fixed points. This gives some special properties on phase diagram of QCD.

14 Ferromagnetism, Bose-Einstein condensation and superconductivity of QED

Let us then investigate the phenomena of superconductivity and magnetism by the above renormalization group method. Let us first consider the Case 1) with $0 < \epsilon \ll 1$ for the three dimensional space statistics. For satisfying the inequality (88) of this case from the formula for B and C we have $h = 0$ or $\kappa = 0$. Let us first consider the case $h = 0$. For this subcase we have that the equation (89) also trivially holds. Then the inequality (88) is simplified to the following equality:

$$-2 + \frac{1}{64\kappa^{12}} > 0\tag{104}$$

This gives an estimate of the critical value κ_c of κ :

$$2^{-\frac{7}{12}} > \kappa_c\tag{105}$$

Let us identify the constant κ as a constant proportional to the absolute temperature T such that $\kappa = k_B T$ where k_B denotes the Boltzmann constant. Since $h = 0$ gives the ground state of electrons we have that $\kappa > 0$ gives the static magnetic property of the ground state of electrons. Moreover since $h \neq 0$ gives dynamical effect we have that $h = 0$ and $\kappa > 0$ gives the static magnetic property. Thus this subcase can be identified as a static magnetic phase transition where $\kappa_c = k_B T_c$ and T_c is as the critical temperature for the magnetic phase transition.

Moreover from the winding numbers of the photon loops we have that the sign \pm of $\pm h \neq 0$ gives the two opposite spins of photons and of electrons. Thus the dynamical interaction of spins is from $\pm h \neq 0$.

Then when $h = 0$ there is no dynamical interaction among the spins. In this case the antiferromagnetic phase does not appear since antiferromagnetism is formed by the dynamical interaction of two spins with opposite signs. Thus this static magnetic phase transition given by this case $h = 0$ and $\kappa > 0$ is the ferromagnetic phase transition where the paramagnetic phase is transitioned to the ferromagnetic phase when the temperature T is decreased from $T > T_c$ to $T < T_c$.

Let us then consider the subcase that $h \neq 0$ and $\kappa = 0$. We shall show that this subcase can be identified as the Bose-Einstein condensation and is related to the Type I superconductivity. For this subcase $h \neq 0$ and $\kappa = 0$, the equation (89) always holds. Then the inequality (88) is simplified to the following equality:

$$-2 + \frac{1}{64h^{12}} > 0 \quad (106)$$

This gives a condition for the critical value h_c of h :

$$2^{-\frac{7}{12}} > h_c \quad (107)$$

Then since the critical temperature $\kappa_c = \kappa = 0$ the following subcase:

$$2^{-\frac{7}{12}} > h_c > 0, \quad \kappa_c = 0 \quad (108)$$

can be identified as the Bose-Einstein condensation.

Let us extend this case (108) to that $\kappa \approx 0$ but is not equal to zero. Let us find out such a range for $h \neq 0$ and $\kappa \approx 0$. This range is then as the phase of (Type I) superconductivity. First we must have that $h > \kappa$. Then we have:

$$\begin{aligned} CB^2 &= 2^{-6} \frac{1}{(ih+\kappa)^{12}} = 2^{-6} [(\bar{\kappa}^3 - 3\bar{\kappa}\bar{h}^2 + 3\bar{\kappa}^2\bar{h} - \bar{h}^3)^2 \times \\ &\times (\bar{\kappa}^3 - 3\bar{\kappa}\bar{h}^2 - 3\bar{\kappa}^2\bar{h} + \bar{h}^3)^2 - 4\bar{\kappa}^2\bar{h}^2(\bar{h}^2 - 3\bar{\kappa}^2)^2(\bar{\kappa}^2 - 3\bar{h}^2)^2] \\ &+ i2^{-6} \cdot 4\bar{\kappa}\bar{h}(\bar{\kappa}^3 - 3\bar{\kappa}\bar{h}^2 + 3\bar{\kappa}^2\bar{h} - \bar{h}^3)(\bar{\kappa}^3 - 3\bar{\kappa}\bar{h}^2 - 3\bar{\kappa}^2\bar{h} + \bar{h}^3)(\bar{h}^2 - 3\bar{\kappa}^2)(\bar{\kappa}^2 - 3\bar{h}^2) \end{aligned} \quad (109)$$

Thus for (92) holds we must have the condition $\kappa = 0$ or the following condition:

$$h^2 = 3\kappa^2 \quad (110)$$

The condition (110) will be as the basic state of superconductivity.

These two conditions are of the same kind for (92) holds. Then when h_c is very small we have that these two states $\kappa_c = 0$ and $h_c^2 = 3\kappa_c^2$ are closed to each other. Thus when h_c is very small, the range for $\kappa_c \approx 0$ is $0 \leq \kappa_c \leq 3^{-\frac{1}{2}}h_c$ where $h_c < 2^{-\frac{7}{12}}$. Thus the range of the phase of superconductivity (which will be of Type I) is included in the following range:

$$0 \leq \kappa_c \leq \frac{1}{\sqrt{3}}h_c \quad \text{and} \quad 0 < h_c < 2^{-\frac{7}{12}} \quad (111)$$

where $\kappa_c = k_B T_c$ and T_c is as the critical temperature for (Type I) superconductivity. We shall later find out the exact range of Type I superconductivity.

For a fixed $\kappa_c > 0$, the condition $h^2 = 3\kappa_c^2$ will be as the basic state of superconductivity and the condition $h^2 > 3\kappa_c^2$ will be as the normal metallic state. Then we shall show that the Cooper pair of electrons with different spins is as a mechanism of reducing h for the transition from the normal metallic state to the state of superconductivity. Briefly, in the normal metallic state the two electrons of a Cooper pair are described by two phases $e^{\pm ih}$. Then the different sign of $\pm ih$ gives the effect of reducing h for the transition from the normal metallic state to the state of superconductivity. We shall give more details of the mechanism of Cooper pair for reaching the state of superconductivity.

We remark that it may be the case that the state $h^2 = 3\kappa_c^2$ can be reached without the forming of Cooper pairs. In this case the state $h^2 = 3\kappa_c^2$ gives phenomenon which is similar but is different from the usual phenomenon of superconductivity with the Cooper pair mechanism. In this paper we shall only investigate the case of the usual superconductivity with the Cooper pair mechanism.

Thus when $0 < h_c < 2^{-\frac{7}{12}}$ and $h_c^2 = 3\kappa_c^2$ (such that h_c and κ_c are very small) we have the following formula for the critical temperature T_c :

$$k_B T_c = \kappa_c = \frac{1}{\sqrt{3}} h_c =: \frac{1}{\sqrt{3}} \Delta(0) =: \frac{1}{\sqrt{3}} \bar{h}_c \omega_D \quad (112)$$

where $\Delta(0) := h_c$ is as the energy gap of a Cooper pair of electrons and ω_D denotes the Debye frequency of the phonons and \bar{h}_c denotes a value of the Planck constant parameter h such that $\bar{h}_c \omega_D = h_c$. Thus this formula (112) represents the critical temperature T_c in terms of the energy gap $\Delta(0)$.

We notice that when h_c is further restricted such that \bar{h} is the usual Planck constant (divided by 2π) this formula (112) of the critical temperature T_c is of the same form as the formula of the critical temperature T_c in the BCS theory. Here the coefficient $\frac{1}{\sqrt{3}} = \frac{2}{3.4641}$ is close to the corresponding coefficient $\frac{2}{3.5}$ of the formula of the critical temperature T_c in the BCS theory [21, 22, 23, 24, 25, 26].

As the BCS theory because ω_D is proportional to $M^{-\frac{1}{2}}$ where M denotes the mass of the isotope of the material in the phase of superconductivity, the formula (112) gives the isotope effect [21, 22, 23, 24, 25, 26].

15 Conventional Type I and Type II superconductivity of QED

Let us then consider the subcase that $h \neq 0$ and $\kappa > 0$ of the Case 1) with the three dimensional space statistics ($0 < \epsilon \ll 1$). We shall show that this subcase gives the conventional Type II superconductivity (When $\kappa > 0$ is very small, this subcase also gives the Type I superconductivity). For this subcase $h \neq 0$ and $\kappa > 0$, from (109), the condition (88) can be written in the following form:

$$\begin{aligned} & [(\bar{\kappa}^3 - 3\bar{\kappa}\bar{h}^2 + 3\bar{\kappa}^2\bar{h} - \bar{h}^3)^2(\bar{\kappa}^3 - 3\bar{\kappa}\bar{h}^2 - 3\bar{\kappa}^2\bar{h} + \bar{h}^3)^2 \\ & - 4\bar{\kappa}^2\bar{h}^2(\bar{h}^2 - 3\bar{\kappa}^2)^2(\bar{\kappa}^2 - 3\bar{h}^2)^2] > 2 \cdot 2^6 \end{aligned} \quad (113)$$

Then from (109), the condition (92) can be written in the following form:

$$(\bar{h}^2 - 3\bar{\kappa}^2)(\bar{\kappa}^2 - 3\bar{h}^2) = 0 \quad (114)$$

Then from (114) we have that the inequality (88) (or (113)) is of the following form:

$$(\bar{\kappa}^3 - 3\bar{\kappa}\bar{h}^2 + 3\bar{\kappa}^2\bar{h} - \bar{h}^3)^2(\bar{\kappa}^3 - 3\bar{\kappa}\bar{h}^2 - 3\bar{\kappa}^2\bar{h} + \bar{h}^3)^2 > 2^7 \quad (115)$$

where $0 < \bar{\kappa} < 1$ and $0 < \bar{h} < 1$. Then from (114) we have the following two subcases:

$$h^2 - 3\kappa^2 = 0 \quad (116)$$

$$\kappa^2 - 3h^2 = 0 \quad (117)$$

Since the subcase (116) gives $h^2 > \kappa^2$, this subcase (116) is identified as the state of the conventional Type II (and Type I) superconductivity. On the other hand the subcase (117) gives $h^2 < \kappa^2$. Thus this subcase is for magnetic phase transition, as the above case of ferromagnetism. Now since $h^2 \neq 0$ gives the dynamical interaction of up and down spins specified by the \pm of $\pm ih$, we have that this subcase can be identified as the state of the (conventional) antiferromagnetism.

For the subcase (116), the inequality (115) is simplified to the following inequality:

$$2^{-6} 2^{12} \bar{\kappa}^{12} = \frac{2^6}{2^{24} \bar{\kappa}^{12}} = \frac{1}{2^{18} \bar{\kappa}^{12}} > 2 \quad (118)$$

This gives the condition on the parameter κ (and the parameter $h^2 = 3\kappa^2$) for the phase transition of the conventional Type II (and Type I) superconductivity. We can write this condition in the following form:

$$\frac{\sqrt{3}}{2} \cdot 2^{-\frac{7}{12}} > h_c \quad (119)$$

where we let $h = h_c$ and $h_c^2 = 3\kappa^2$.

For the subcase (117), the inequality (115) is simplified to the following inequality:

$$2^{-6}2^{12}\bar{h}^{12} = 2^6 \frac{2^6}{2^{24}\bar{h}^{12}} = \frac{1}{2^{18}\bar{h}^{12}} > 2 \quad (120)$$

This gives the condition on the parameter h for the (conventional) antiferromagnetism. We can write this condition in the following form (we let $h = h_c$):

$$h_{cAmax} := \frac{1}{2} \cdot 2^{-\frac{7}{12}} > h_c \quad (121)$$

Let us then consider the following condition for satisfying (92):

$$(\bar{\kappa}^3 - 3\bar{\kappa}\bar{h}^2 + 3\bar{\kappa}^2\bar{h} - \bar{h}^3)(\bar{\kappa}^3 - 3\bar{\kappa}\bar{h}^2 - 3\bar{\kappa}^2\bar{h} + \bar{h}^3) = 0 \quad (122)$$

This condition can be simplified to the following conditions:

$$\kappa^2 = h^2; \quad \text{or} \quad \kappa^2 = (2 \pm \sqrt{3})^2 h^2 \quad (123)$$

The conditions (123) can also be written in the following form:

$$\kappa^2 = h^2; \quad \text{or} \quad h^2 = (2 \pm \sqrt{3})^2 \kappa^2 \quad (124)$$

These conditions are as further states of phase transitions. We remark that because these further states of phase transitions are different from the above states of phase transitions of antiferromagnetism and conventional superconductivity we shall also call these further states of phase transitions as the states of cross-over.

The two states $h > 0, \kappa = 0$ and $h^2 = 3\kappa^2 > 0$ are as states of superconductivity when h is restricted by the condition (119). Thus for a fixed h_c such that $h_c < \frac{\sqrt{3}}{2} \cdot 2^{-\frac{7}{12}}$, the range $0 < \kappa^2 \leq \frac{1}{3}h_c^2$ is between two states of superconductivity.

The state $\frac{1}{(2+\sqrt{3})^2}h^2 = \kappa^2$ is a state of phase transition. Thus, when the temperature is decreasing (or when the field is cooled) the material is from the state of superconductivity $\frac{1}{3}h^2 = \kappa^2$ tending to the state $\frac{1}{(2+\sqrt{3})^2}h^2 = \kappa^2$.

Let h_{cI} and h_{cII} be two h values related by $\frac{1}{3}h_{cI}^2 = \frac{1}{(2+\sqrt{3})^2}h_{cII}^2$. From this relation let us define a critical value h_{cImax} by:

$$h_{cImax} := \frac{\sqrt{3}}{2 + \sqrt{3}} \frac{\sqrt{3}}{2} \cdot 2^{-\frac{7}{12}} \quad (125)$$

Then the region of Type I superconductivity is the following region:

$$\frac{1}{(2 + \sqrt{3})^2}h_{cI}^2 < \kappa^2 \leq \frac{1}{3}h_{cI}^2; \quad 0 < h_{cI} < h_{cImax}. \quad (126)$$

Then let us define a critical value h_{cIImax} by:

$$h_{cIImax} := \frac{\sqrt{3}}{2} \cdot 2^{-\frac{7}{12}} \quad (127)$$

Then the region of Type II superconductivity is the following region:

$$\frac{1}{(2 + \sqrt{3})^2}h_{cII}^2 < \kappa^2 \leq \frac{1}{3}h_{cII}^2; \quad h_{cImax} \leq h_{cII} < h_{cIImax}. \quad (128)$$

where the range of κ is connected with the corresponding range of κ of the Type I superconductivity by the relation of h_{cI} and h_{cII} . We remark that the critical values h_{cImax} and h_{cIImax} correspond to the critical magnetic field strength H_{c1} and H_{c2} of the Ginzberg-Landau model of superconductivity.

15.1 Meissner effect

In the above sections we show that the magnetic properties are from the photon loops. When a material is in the phase of Type I superconductivity with the Cooper pair mechanism, the spins (which are determined by the photon loops with the phases $e^{\pm ih}$ where $h \neq 0$) of the two electrons of a Cooper pair are opposite to each other. Thus the net magnetic fluxes of the two photon loops of the two electrons of a Cooper pair is equal to 0. Further, when a material is in the state of Type I superconductivity, the photons (or loops of photon) in this material had to be attached to (or absorbed by) the Cooper pairs of electrons to form pairs with spins opposite to each other. Thus, in the state of Type I superconductivity, the net numbers of loops of photons (and electrons) is equal to 0. Then since an external magnetic field acting on a material is as a set of loops of photons in this material, when this material is in the state of Type I superconductivity we have that the net winding numbers of loops of photons (and electrons) is equal to 0. Thus an external magnetic field acting on a material gives the zero effect of the net winding numbers of loops of photons in this material when this material is remained in the state of Type I superconductivity under the action of the external field. Thus the external magnetic field is expelled from this material in the state of Type I superconductivity. Thus we have the Meissner effect.

We remark that in the case that the state $h^2 = 3\kappa_c^2$ is reached without the Cooper pair mechanism then we may not have the Meissner effect. In this case we have the phenomenon of persistent current (which is a phenomenon of superconductivity) appearing in a normal metal which is without the Meissner effect. Such phenomenon of persistent current was experimentally observed [27, 28, 29, 30, 31].

The region of Type I and Type II superconductivity is the following region:

$$\frac{1}{(2 + \sqrt{3})^2} h_c^2 < \kappa^2 \leq \frac{1}{3} h_c^2 \quad \text{and} \quad 0 < h_c < h_{cII\max}. \quad (129)$$

We notice that in this region the parameter $\kappa > 0$ gives static spins for magnetic effect as that of the state for antiferromagnetism. Then this region is with larger h_c^2 (for a fixed κ) than the state for antiferromagnetism. Since h_c^2 gives dynamical effect for spins we have that this region is with more dynamical effect for spins than the state for antiferromagnetism. This dynamical effect for spins weakens the effect of antiferromagnetism which suppresses the net winding number of loops of photons. This gives the Meissner effect in the region of Type I superconductivity where h_c is restricted by the condition $h_c \leq h_{cI\max} < h_{cA\max}$ that the effect of weakening the suppression of the net winding number of loops of photons, is not strong to give the Meissner effect.

On the other hand in the region of Type II superconductivity where h_c is given by the condition $h_{cI\max} \leq h_c < h_{cII\max}$ that the effect of weakening the suppression of the net winding number of loops of photons is stronger. In particular h_c can be large such that $h_{cA\max} < h_c < h_{cII\max}$ since $h_{cA\max} < h_{cII\max}$.

Thus by the effect of weakening the suppression of the net winding number of loops of photons, the effect of winding number of loops of photons can appear in the region of Type II superconductivity when an external magnetic field is applied. This gives the phenomenon of the mixed state of Meissner effect with the appearing of loops of photons in this region of Type II superconductivity (We shall give more analysis on this mixed state in the following section on high- T_c superconductivity where the Type II superconductivity and the high- T_c superconductivity are unified). Since photons are in loop form, in the mixed state when external magnetic field penetrating the material in the state of superconductivity, the loops of photon with the same orientation (or spin) of the magnetic field when attaching together form the macroscopic observable vortices (or magnetic fluxes). These quantum loops of photons give the following formula of the winding numbers which are as the quantization of energy of photons:

$$neq_{min} := n \cdot n_e e_0 \cdot \frac{n_m e_0 \pi}{k_0}, \quad (130)$$

for $n = 0, 1, 2, 3, \dots$. When these loops of photons (with the same winding number) attaching together giving the macroscopic vortices, these vortices are with the same winding numbers and thus are with the following quantum of magnetic fluxes:

$$n\Phi_0 := n \frac{h_0}{2e} := neq_{min} := n \cdot n_e e_0 \cdot \frac{n_m e_0 \pi}{k_0} \quad (131)$$

for $n = 0, 1, 2, 3, \dots$, where $\Phi_0 := \frac{h_0}{2e} := \frac{q_{min}}{2}$ is the unit of magnetic flux.

Thus from the quantization of loops of photons, we have the phenomenon of quantization of the vortices. We shall give more description of the possibility of appearance of vortices in the following section on high- T_c superconductivity. ¶

From the above region of Type I superconductivity, as the temperature decreasing (or the field is cooled) to the state $\frac{1}{(2+\sqrt{3})^2}h_{cI}^2 = \kappa^2$ we have a phase transition (or cross-over). Crossing this state we have that $h_{cI}^2 > (2 + \sqrt{3})^2 \kappa^2$. Thus crossing this state the spins of electrons are with more dynamical effect than the region of Meissner effect. In this case the antiferromagnetic state of the spins of the electrons becomes a state which is more dynamical. Since the state of paramagnetic Meissner effect is with more dynamical effect than that of the antiferromagnetic state and the Type I superconductivity we have that the range of κ of paramagnetic Meissner effect is the following range:

$$0 < \kappa^2 \leq \frac{1}{(2 + \sqrt{3})^2} h_{cI}^2 \quad (132)$$

In addition, we have the following condition:

$$0 < h_{cI} < h_{cI_{max}} \quad (133)$$

These two conditions give the region of paramagnetic Meissner effect which is connected to the region of Type I superconductivity. We shall in the next section give the phase figures of the regions of the Type I and Type II superconductivity and the paramagnetic Meissner effect when we investigate the phase diagram of high- T_c superconductivity. Experimentally the phenomenon of conventional paramagnetic Meissner effect was observed [32, 33]. We shall also consider the unconventional paramagnetic Meissner effect which was observed before the conventional paramagnetic Meissner effect [34, 35, 36, 37, 38].

Symmetric to the range $\frac{1}{(2+\sqrt{3})^2}h_c^2 < \kappa^2 \leq \frac{1}{3}h_c^2$ (the range of Meissner effect with vortex phenomena) which is a diamagnetic effect, the following range of κ :

$$(2 + \sqrt{3})^2 h_c^2 > \kappa^2 \geq 3h_c^2 \quad (134)$$

is the range of antiferromagnetism, which is a property similar to that of diamagnetism, for a fixed h_c such that $\frac{1}{2} \cdot 2^{-\frac{7}{12}} > h_c$.

Then symmetric to the range $0 < \kappa^2 \leq \frac{1}{(2+\sqrt{3})^2}h_{cI}^2$ (the range of paramagnetic Meissner effect) which is of paramagnetic effect, the following range of κ :

$$\kappa^2 \geq (2 + \sqrt{3})^2 h_c^2 \quad (135)$$

is the range of paramagnetism, for a fixed h_c such that $\frac{1}{2} \cdot 2^{-\frac{7}{12}} > h_c$. Thus the state $\kappa^2 = (2 + \sqrt{3})^2 h_c^2$ is the state for the phase transition of paramagnetism transited to antiferromagnetism as κ^2 decreasing, for a fixed h_c such that $\frac{1}{2} \cdot 2^{-\frac{7}{12}} > h_c$.

Then as κ decreasing the next state is $\kappa^2 = 3h_c^2$ which is the state for the phase transition of antiferromagnetism transited to another phase. Following this state is the state $\kappa^2 = h_c^2$ which is a symmetric state of κ and h where κ is for static spin effect and h is for dynamical wave effect. Thus the following range of κ :

$$3h_c^2 > \kappa^2 > h_c^2 \quad (136)$$

is identified as the phase of spin density waves where κ gives static spin effect, h gives wave and (charge) effect and that $\kappa^2 > h_c^2$ indicates that the ratio of spin effect is greater than charge effect, and thus is the property of spin density waves (in contrast to charge density waves), for a fixed h_c such that $\frac{1}{2} \cdot 2^{-\frac{7}{12}} > h_c$. In this 3D Case 1), this phase of spin density waves is identified as the phase of spin density waves in spin glass form. Then as a symmetry the following range of κ :

$$h_c^2 > \kappa^2 > \frac{1}{3}h_c^2 \quad (137)$$

is identified as the phase of charge density waves, where $h_c^2 > \kappa^2$ indicates that the ratio of spin effect is less than charge effect, and thus is the property of charge density waves (in contrast to spin density waves), for a fixed h_c such that $\frac{\sqrt{3}}{2} \cdot 2^{-\frac{7}{12}} > h_c$. (Since this phase of charge density waves is a phase of more charge effect, the condition $\frac{\sqrt{3}}{2} \cdot 2^{-\frac{7}{12}} > h_c$ which is with larger h_c for charge effect and is the condition for superconductivity is used instead of the condition $\frac{1}{2} \cdot 2^{-\frac{7}{12}} > h_c$ for antiferromagnetism). In this 3D Case 1), this phase of charge density waves is identified as the phase of charge density waves in spin glass form. Then the state $\kappa^2 = h_c^2$ is the state of phase transition (or cross-over) for the phase of spin density waves transited to the phase of charge density waves, as κ decreasing.

On the other hand since the range (136) of spin density waves can be identified as a range of insulator and the range (137) of charge density waves can be identified as a range of semiconductor, the state $\kappa^2 = h_c^2$ is also the state of phase transition for the phase of insulator transited to the phase of conductor, as κ decreasing.

16 High- T_c superconductivity of QED

Let us then consider the 2D Case 2) with $\epsilon = 1$. For this case we have the subcase that $h_c \neq 0$ and $\kappa_c > 0$. We have that (91) is of the following form:

$$\text{Re}(i\bar{h} + \bar{\kappa})^{12} > 0 \quad (138)$$

where $0 \leq \bar{h}, \bar{\kappa} \leq 1$. Also we have that (92) is of the following form:

$$\text{Im}(i\bar{h} + \bar{\kappa})^{12} = 0 \quad (139)$$

As similar to the above Case 1) from (139) we have the following condition:

$$(h^2 - 3\kappa^2)(\kappa^2 - 3h^2) = 0 \quad (140)$$

This gives the following conditions:

$$h^2 - 3\kappa^2 = 0 \quad (141)$$

$$\kappa^2 - 3h^2 = 0 \quad (142)$$

Remark. In this Case 2) for the two subcases $h = 0$ and $\kappa = 0$ we also get conditions similar to (141) and (142). However these conditions do not give restrictions on h or κ to give conditions of phases. Thus the two subcases $h = 0$ and $\kappa = 0$ do not give more phases and thus can be omitted. \blacktriangledown

From (141) we have that (138) is simplified to the following condition:

$$\frac{1}{2^{18}\kappa^{12}} > 0 \quad (143)$$

Unlike the corresponding condition in the Case 1) this condition always hold for $\kappa > 0$. Thus for $\epsilon = 1$ the parameter $\kappa > 0$ can be large such that the critical temperature T_c can be very high. This corresponds to the high- T_c superconductivity phase transition. On the other hand from (142) we have that (138) is simplified to the following condition:

$$\frac{1}{2^{18}h^{12}} > 0 \quad (144)$$

Unlike the corresponding condition in the Case 1) this condition always holds for $h \neq 0$. Thus for $\epsilon = 1$ the parameter $h \neq 0$ (and the parameter $\kappa^2 = 3h^2$) can be large such that the critical temperature T_N for antiferromagnetism can be high.

As Case 1) let us then consider the following condition from which (138) holds:

$$(\bar{\kappa}^3 - 3\bar{\kappa}\bar{h}^2 + 3\bar{\kappa}^2\bar{h} - \bar{h}^3)(\bar{\kappa}^3 - 3\bar{\kappa}\bar{h}^2 - 3\bar{\kappa}^2\bar{h} + \bar{h}^3) = 0 \quad (145)$$

This condition can be simplified to the following conditions:

$$h^2 = \kappa^2; \quad \text{or} \quad h^2 = (2 \pm \sqrt{3})^2 \kappa^2 \quad (146)$$

Each of these conditions gives a state of phase transition.

We notice that the two states (141) and (142) of superconductivity and antiferromagnetism are as phases of superconductivity and antiferromagnetism which are one dimensional lines (and not as two dimensional regions) in the two dimensional phase plane (κ, h) . Thus these two phases will be unstable. However when the two dimensional phase plane (κ, h) is transformed to the two dimensional phase plane (T, x) of the cuprates where x denotes the doping parameter, a part of the phase line (141) of superconductivity is bifurcated into two lines which encompass a region (We shall show the existence of this bifurcation and the forming of the region). Similarly the region of antiferromagnetism is also formed by such bifurcation of phase line. These two regions are then the two well known regions of superconductivity and antiferromagnetism in the well known phase diagram in the phase plane (T, x) of the cuprates [43, 44, 45]. In forming these two regions the width of each of the two regions is the length of the coordinate x . In forming the region of superconductivity when κ (or T) is fixed we have that the parameter h is also fixed by the equation $h^2 = 3\kappa^2$. Then as the doping parameter x ranging from one end of the region to another end of the region, the corresponding parameter h (which corresponds to the variation of x) is kept to be fixed by the equation $h^2 = 3\kappa^2$. This then has the effect that the phase line $h^2 = 3\kappa_c^2$ is bifurcated into two lines to form the region of superconductivity in the phase plane (T, x) .

Similarly the region of antiferromagnetism in the phase plane (T, x) is formed in this way. This then give the existence of the two phases of superconductivity and antiferromagnetism in the phase plane (T, x) of the cuprates [43, 44, 45].

Let us then show the existence of the bifurcation of phase line and the forming of 2D phase region. Let us consider the case of superconductivity. For the conventional Type II superconductivity we have the following range of superconductivity:

$$\frac{1}{3}h^2 \geq \kappa^2 > (2 - \sqrt{3})^2 h^2 \quad (147)$$

for a fixed h such that $h_{cI\max} \leq h < h_{cII\max}$. Then since the conventional Type II superconductivity is as a part of the complete region of superconductivity we have that this range give a range in the region of superconductivity. This range is as a part of the maximal range in the axis of x of the complete region of superconductivity. This thus give a nonempty region of superconductivity and the existence of bifurcation for forming this region. This shows the existence of bifurcation and the forming of the 2D region of high- T_c (and Type II) superconductivity.

Similarly we can show the existence of the bifurcation and the formation of the 2D region of antiferromagnetism.

16.1 Meissner effect with quantized vortex phenomenon

We have shown that the existence of the conventional Type II superconductivity gives the bifurcation of the phase line $h^2 = 3\kappa_c^2$ of superconductivity and this bifurcation gives the stable existence of the region of high- T_c superconductivity. When bifurcation forming the region of high- T_c superconductivity, this region of high- T_c superconductivity is from the left bifurcation phase line $h^2 = 3\kappa_c^2$ of superconductivity to the right bifurcation phase line $h^2 = 3\kappa_c^2$ of superconductivity. This region of high- T_c superconductivity is just above (and contains) the region of the conventional Type II superconductivity. Thus the region of high- T_c superconductivity and the conventional Type II superconductivity are both formed by the phase line $h^2 = 3\kappa_c^2$. Further for the high- T_c superconductivity since the region of high- T_c superconductivity is above the region of conventional Type II superconductivity there exists h of the phase line $h^2 = 3\kappa_c^2$ such that $h_{cA\max} < h$. Thus as the conventional Type II superconductivity the Meissner effect with vortex phenomenon may appear in the region of high- T_c superconductivity. Moreover, since the unified region of high- T_c superconductivity and the conventional Type II superconductivity is formed by the bifurcation of the phase line $h^2 = 3\kappa_c^2$, this unified region is easier to be penetrated by the magnetic fluxes of external magnetic field. Thus the mixed state of the Meissner effect with vortex phenomenon is easier to appear in this unified region. Then as the case of the conventional Type II superconductivity, the vortices are from photon loops and are with the winding number as quantization and thus are with the following

quantum of magnetic fluxes:

$$n\Phi_0 := n \frac{h_0}{2e} := neq_{min} := n \cdot n_e e_0 \cdot \frac{n_m e_0 \pi}{k_0}, \quad (148)$$

for $n = 0, 1, 2, 3, \dots$, where $\Phi_0 := \frac{h_0}{2e} := \frac{q_{min}}{2}$ is the unit of magnetic flux. Thus we have the quantization of the vortex phenomenon. ¶

For a fixed κ_c the range $3\kappa_c^2 < h^2$ is separated into two ranges $3\kappa_c^2 < h^2 < (2 + \sqrt{3})^2 \kappa_c^2$ and $(2 + \sqrt{3})^2 \kappa_c^2 \leq h^2$. Crossing the state $h^2 = 3\kappa_c^2$ of Meissner effect, the spins of electrons are with more dynamical effect than the range of Meissner effect. In this case the antiferromagnetic state of the spins of the electrons become the paramagnetic state which is more chaotic. In this case, the Meissner effect becomes a paramagnetic Meissner effect [34, 35, 36, 37, 38]. Thus the following range:

$$3\kappa_c^2 < h^2 < (2 + \sqrt{3})^2 \kappa_c^2 \quad (149)$$

is the range of paramagnetic Meissner effect. We remark that at the crossing of the state $h^2 = 3\kappa_c^2$ if we let h^2 be fixed and let κ_c decreasing to 0 (or the field is cooled) we also get the effect of the transition from Meissner effect to paramagnetic Meissner effect [34, 35, 36, 37, 38].

Then the next state $h^2 = (2 + \sqrt{3})^2 \kappa_c^2$ is a state of phase transition. Crossing this state we have $(2 + \sqrt{3})^2 \kappa_c^2 < h^2$. Thus crossing this state the spins of electrons are with more dynamical effect than the range of paramagnetic Meissner effect. In this case the antiferromagnetic state of the spins of the electrons become the normal metallic state which is more chaotic. In this case, the paramagnetic Meissner effect becomes the normal metallic effect. Thus the following range:

$$(2 + \sqrt{3})\kappa_c^2 < h^2 \quad (150)$$

is the range of normal metallic state.

As a symmetry to that the range $3\kappa_c^2 < h^2 < (2 + \sqrt{3})^2 \kappa_c^2$ is the range of paramagnetic Meissner effect we have that the following range of h^2 :

$$\frac{1}{(2 + \sqrt{3})^2} \kappa_c^2 < h^2 < \frac{1}{3} \kappa_c^2 \quad (151)$$

is the range of paramagnetism.

Then as a symmetry to that the range $h^2 > (2 + \sqrt{3})^2 \kappa_c^2$ is the range of normal metallic state, the following range of h^2 :

$$0 < h^2 < \frac{1}{(2 + \sqrt{3})^2} \kappa_c^2 \quad (152)$$

is the range of diamagnetism, for an (arbitrary) fixed κ_c . Thus the state $h^2 = \frac{1}{(2 + \sqrt{3})^2} \kappa_c^2$ is the state of phase transition (or cross-over) from diamagnetism transited to paramagnetism as h^2 increasing.

Then as h^2 increasing the next state is $\kappa_c^2 = 3h^2$ which is the state of phase transition for the phase (or state) of antiferromagnetism transited to the phase of spin density waves. Following this state is the state $\kappa_c^2 = h^2$. Thus the following range of h^2 :

$$\frac{1}{3} \kappa_c^2 < h^2 < \kappa_c^2 \quad (153)$$

is the range of spin density waves, for a fixed κ_c . Then the following range of h^2 :

$$\kappa_c^2 < h^2 < 3\kappa_c^2 \quad (154)$$

is as the (first range) of charge density waves, for a fixed κ_c (We remark that the above range of paramagnetic Meissner effect can be regarded as the second range of charge density waves). Thus the state $h^2 = \kappa_c^2$ is as the state of phase transition for the phase of spin density waves transited to the phase of charge density waves, where $\kappa_c > 0$ is for static spins while $h \neq 0$ is for dynamical charge. We remark

that the range of spin density waves and charge density waves is also called the range of pseudogap. This identification of the range of spin density waves and charge density waves agrees with experimental results [39, 40, 41, 42].

As the Case 1) the state $h^2 = \kappa_c^2$ is also as the state of phase transition for the phase of Mott insulator transited to the phase of semiconductor, where the phase (153) of spin density waves is a phase of Mott insulator and the phase (154) of charge density waves is a phase of semiconductor.

16.2 The condition (113) as condition of 3D phase in the complete phase diagram of high- T_c superconductivity

We notice that the condition (113) in the above section on conventional Type II superconductivity divides the phase diagram of material with high- T_c superconductivity into two phases. The phase satisfies the condition (113) is for the phase diagram in the above section including the conventional Type II superconductivity which is identified as the low- T_c phase appearing in the bottom of the phase diagram of cuprates such as the cuprate $La_{2-x}Sr_xCuO_4$ [43, 44, 45].

Then the other phase of the phase diagram of high- T_c superconductivity satisfies the following condition which is complementary to the condition (113):

$$\begin{aligned} & [(\bar{\kappa}^3 - 3\bar{\kappa}\bar{h}^2 + 3\bar{\kappa}^2\bar{h} - \bar{h}^3)^2(\bar{\kappa}^3 - 3\bar{\kappa}\bar{h}^2 - 3\bar{\kappa}^2\bar{h} + \bar{h}^3)^2 \\ & - 4\bar{\kappa}^2\bar{h}^2(\bar{h}^2 - 3\bar{\kappa}^2)^2(\bar{\kappa}^2 - 3\bar{h}^2)^2] \leq 2^7 \end{aligned} \quad (155)$$

This phase is the main phase in the upper high- T_c part of the phase diagram of material with high- T_c superconductivity such as the cuprate $La_{2-x}Sr_xCuO_4$.

We notice that the conventional Type II superconductivity is of three dimensional space nature (with $0 < \epsilon \ll 1$) while high- T_c superconductivity is of two dimensional space nature (with $\epsilon = 1$). Thus the two phases specified by the condition (155) and the condition (113) give a dimensional crossover. Such a phase diagram agrees with the fact that the cuprates such as $La_{2-x}Sr_xCuO_4$ are quasi 2D materials which are 3D materials but are with 2D properties in the experiments of superconductivity. Thus the conventional Type II superconductivity is a phase in the 3D phase and is as the 3D phase part of the complete phase of high- T_c superconductivity. ¶

Since any point (κ, h) of the phase line $h^2 = 3\kappa^2$ of superconductivity can be the bifurcation point and that there is no upper bound on h for the high- T_c superconductivity we have that there is no upper limit on the critical temperature T_c of high- T_c superconductivity. From the above phase diagram we see that the increasing of h corresponds to the increasing of the parameter x of cuprates [43, 44, 45]. Thus the changing of the Planck constant parameter h can be achieved by methods such as doping of cuprates.

16.3 Phase diagram of $La_{2-x}Sr_xCuO_4$

As an example let us consider the experiments of the cuprate $La_{2-x}Sr_xCuO_4$ [43, 44, 45]. Let us consider the (T, x) phase diagram of $La_{2-x}Sr_xCuO_4$ in Fig.1 (This phase diagram is derived from the well known experimental (T, x) phase diagram of $La_{2-x}Sr_xCuO_4$ [43, 44, 45]).

In this phase diagram the parameter κ corresponds to T by the relation $\kappa = k_B T$. The line **a** denotes the phase line $\kappa^2 = 3h^2$ (of the phase plane (κ, h)) in the phase plane (T, x) . The line **b** denotes the cross-over line $\kappa^2 = h^2$ (of the phase plane (κ, h)) in the phase plane (T, x) . The line **c** denotes the phase line $h^2 = 3\kappa^2$ (of the phase plane (κ, h)) of superconductivity in the phase plane (T, x) . Then the line **d** denotes the cross-over line $h^2 = (2 + \sqrt{3})^2 \kappa^2$ (of the phase plane (κ, h)) in the phase plane (T, x) . In this phase diagram the original phase line $h^2 = 3\kappa^2$ with the part denoted by the dash line is bifurcated into the phase line $h^2 = 3\kappa^2$ denoted by the line **c** in the phase plane (T, x) .

The two lines **a** and **c** are the two basic phase lines for antiferromagnetism and superconductivity respectively in the well known (T, x) phase diagram of $La_{2-x}Sr_xCuO_4$ [43, 44, 45]). In the phase diagram in Fig.1 we have two more phase lines **b** and **d**. The region between **a** and **b** is the region of spin density waves and region of insulator. The region between **b** and **c** is the region of charge density waves and

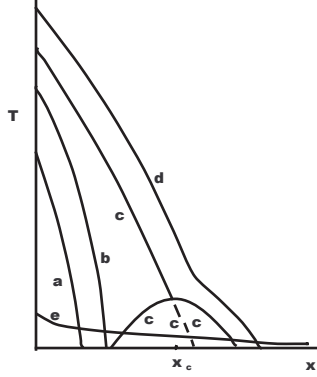


Fig.5. (T, x) phase diagram of $La_{2-x}Sr_xCuO_4$.

In this phase diagram, the line **a** is the (bifurcation) phase line $\kappa^2 = 3h^2$ of antiferromagnetism, the line **b** is the cross-over line $h^2 = \kappa^2$ of insulator to semiconductor, the line **c** is the (bifurcation) phase line $h^2 = 3\kappa^2$ of superconductivity, the line **d** is the cross-over line $h^2 = (2 + \sqrt{3})^2\kappa^2$ of state of pseudogap to normal metallic state; the line **e** is the cross-over line from the phase of 2D to the phase of 3D (which coexists with the phase of 2D).

region of semiconductivity. The region between **a** and **c** is usually called the region of pseudogap. The region between **c** and **d** is the region of paramagnetic Meissner effect and is usually called the region of non-Fermi liquid (We shall also call this region as the extended region of pseudogap. We shall explain more on this extended region of pseudogap). The right side of **d** is the region of normal metallic state. Then the bifurcation of the phase line **c** gives the region of high- T_c superconductivity. Then the left side of **a** is the region of antiferromagnetism (The region of antiferromagnetism is also obtained by the bifurcation of the phase line **a** where a part of this region of antiferromagnetism obtained by bifurcation is at the outside of this phase diagram in Fig.1).

Then let us consider the special phase line **e**. This phase line **e** is the cross-over line from the phase of two dimensional phenomenon (i.e. the Case 2) with $\epsilon = 1$) to the phase of three dimensional phenomenon (i.e. the Case 1) with $0 < \epsilon < 1$). Above this line is the phase of two dimensional phenomenon described in this section on high- T_c superconductivity and below this line is the phase of three dimensional phenomenon described in the above section on conventional Type II superconductivity (This three dimensional phenomenon coexists with the basic two dimensional phenomenon). In this 3D phase the region in the bifurcation region of superconductivity is the region of conventional Type II superconductivity while the region between the line **c** and the line **d** is the region of Type I superconductivity (In the 2D phase this region between the line **c** and the line **d** is the extended region of pseudogap). We remark that in Fig.1 the phase line **e** crosses the phase line **d** with the equation $h^2 = (2 + \sqrt{3})^2\kappa^2$ and decreases to 0 at the right side of the phase line **d**. This is because that the right side of the phase line **d** is the normal metallic state which is at the outside of the phase diagram of conventional Type II superconductivity described in the above section. Furthermore the crossing point is at $\kappa = \frac{1}{(2+\sqrt{3})^2}h^2$, as shown in Fig.1. This is because that in the phase diagram of the conventional Type II superconductivity in the above section, for a given h such that $h_{cI\max} \geq h$, the range of the paramagnetic Meissner effect is the range $\frac{1}{(2+\sqrt{3})^2}h^2 > \kappa^2 > 0$. This gives an exact fitting of the phase diagram of the 3D conventional Type II superconductivity in the phase diagram of the quasi-2D high- T_c superconductivity. Furthermore, since the region of normal metallic state in the vortex core of the conventional superconductivity is the region: $\frac{1}{3}h^2 > \kappa^2 > \frac{1}{(2+\sqrt{3})^2}h^2$ and $h \geq h_{cII\max}$, and the phase diagram of the conventional superconductivity is in the below of the line **e**, we have that in Fig.1 the region of the normal metallic state of

the conventional superconductivity is the region enclosed by the (left) line **c** and the line **e** (and is at the right side of the (left) line **c** and the above of the line **e**). Thus this normal metallic state of the conventional superconductivity in the phase diagram in Fig.1 contains the region of the normal metallic state of the high- T_c superconductivity enclosed by the line **d** and the line **e** (and is at the right side of the line **d** and the above of the line **e**). Thus this phase diagram in Fig.1 is a complete phase diagram on magnetism and superconductivity that it includes the Type I superconductivity, the conventional Type II superconductivity and the high- T_c superconductivity. ¶

16.4 Computation of T_c of $\text{La}_{2-x}\text{Sr}_x\text{CuO}_4$

Let us consider the mechanism of forming Cooper pair for the superconductivity of $\text{La}_{2-x}\text{Sr}_x\text{CuO}_4$. Let us first consider the possibility of superconductivity of the transition element Cu . This element is with the outer shells $3d^{10}4s^1$ of valence electrons. Since Cu is a metal we have that Cu is in the state $\kappa^2 < 3h^2$. For Cu in the state $\kappa^2 = 3h^2$ of superconductivity we have that h^2 is needed to be reduced such that $\kappa^2 = 3h^2$ (It is not that κ^2 is increased such that $\kappa^2 = 3h^2$ because in this case the $|h|$ will be higher than the maximal value h_{IImax} and thus is not in the state of superconductivity). For the decreasing of h let the κ be decreased (or let the temperature T be decreased). In this case we need to have a mechanism for the decreasing of h to reach the state of superconductivity. Let us then consider the Cooper pair of electrons as such a mechanism. Since an atom Cu has only one s electron in the outer shells we have that this s electron can not be used to form a Cooper pair. Thus we can only consider the d electrons in the outer shells of Cu . There are five d electrons with up spins and five d electrons with down spins in the outer shells of Cu . Thus the five d electrons with up spins of one Cu may be with the five d electrons with down spins of another Cu to form five pairs of electrons. Then since the d electrons are in the inner of the outer shells that the binding energy on the d electrons is stronger that such pairings of the d electrons can not be formed stably. Thus for the Cu metal there is no mechanism for the forming of stable pairings of electrons and thus it is difficult for the metal Cu in the state of superconductivity. This agrees with the experiments that Cu is not a superconductor (We remark that Cu being not in the state of superconductivity gives the antiferromagnetic state of La_2CuO_4).

Then let us consider the case of $\text{La}_{2-x}\text{Sr}_x\text{CuO}_4$. We shall show that the interaction of Cu with $\text{La}(\text{Sr})$ opens a channel for the freedom of d valence electrons of Cu by doping $\text{La}(\text{Sr})$. With this channel opening the Cooper pair of d valence electrons between two Cu atoms can be formed by the attractive effect of the seagull vertex interaction. Let the two d electrons for the forming of Cooper pair be with the wave factors $e^{\pm ih_{Cu}}$ respectively in their wave functions where $|h_{Cu}|$ is the energy of the d electrons for the interaction of forming the Cooper pair (The \pm sign is for the up and down spins of the two d electrons. This forms a wave factor $e^{i(h_{Cu}-h_{Cu})}$ of the Cooper pair where $h_{Cu} - h_{Cu} = 0$. This cancelation of energy for the forming of Cooper pair gives the reduction of the energies of the Cu atoms. Thus the forming of Cooper pair is a mechanism for the reduction of energy.

Let us specify the parameter h of $h^2 = 3\kappa^2$. We notice that when there is no mechanism of pairing there is no reduction of h of Cu to let the metal Cu from the normal metallic state to the state of superconductivity. Thus more reduction of energy gives higher critical temperature T_c of superconductivity (when the reduced energy is not exceeded the remained energy). Thus the reduction of energy is proportional to the critical temperature T_c of superconductivity. Let us find out the exact proportion. Each d electron of the metal Cu gives an energy $|h_{Cu}|$. The total energy of d electrons of the metal Cu is $10|h_{Cu}|$. Let h_1 be the energy reduced from this total energy by the mechanism of Cooper pairing. Then since h_1 is proportional to T_c from the state equation of superconductivity we have $h_1^2 = 3\kappa_1^2 = 3(k_B T_{c1})^2$. On the other hand let $h_2 = 10|h_{Cu}| - h_1$ be the energy after the reduction of energy. Then this remained energy must also be proportional to the critical temperature T_c of superconductivity because of the general state equation $h_2^2 = 3\kappa_2^2$ of superconductivity. Thus from the state equation of superconductivity we have $h_2^2 = 3\kappa_2^2 = 3(k_B T_{c2})^2$. Thus from the formula $h^2 = 3\kappa^2$ we have that the maximum of T_c is at the case that h_1 is increased to equal to h_2 . Thus for the maximum of T_c we have $h_1 = h = h_2$. Thus we have the following formula of T_c of $\text{La}_{2-x}\text{Sr}_x\text{CuO}_4$:

$$k_B T_c = \kappa = \frac{1}{\sqrt{3}} \Delta_{LSCO} \quad (156)$$

where $\Delta_{LSCO} = h = 5|h_{Cu}|$ is the energy gap of the high- T_c superconductivity of $La_{2-x}Sr_xCuO_4$ and T_c is the highest critical temperature of superconductivity.

We remark that in the above derivation the energy gap Δ_{LSCO} is from the Cu atom. We shall show that there is a case that a small energy gap $|h_{La(Sr)}|$ from two $La(Sr)$ atoms may appear such that $\Delta_{LSCO} = h = 5|h_{Cu}| + 2|h_{La(Sr)}|$.

Let us then find a way to determine the energy $|h_{Cu}|$. Since the d valence electrons are approximately as free electrons we have that the energy $|h_{Cu}|$ is proportional to the ionization energy of the d electrons. Then since an atom Cu in the CuO_2 plane is vertically interacted with two O atoms in two $La(Sr)O$ planes in opposite directions we have that the d valence electrons of Cu can be in three states of ionization energies. Thus the d valence electrons of Cu can be in the state of third ionization energy of Cu (We shall explain this point in more detail when we consider the effect of $La(Sr)$ on Cu). Thus the maximum value of the energy $|h_{Cu}|$ is proportional to the third ionization energy of Cu (It will be more precise that the maximum value of the energy $|h_{Cu}|$ is proportional to the third ionization energy of the electrons of Cu in the CuO_2 plane. This ionization energy includes the effect of the oxygen atoms on the d electrons).

From the existing table of ionization energy of Cu we have that the third ionization energy of Cu is approximately equal to 3555 kJ/mol. Let $|h_{Cu}| \approx \xi 3555$ kJ/mol where ξ is a proportional constant. We shall show that $\xi \approx 2.83133971 \cdot 10^{-5}$ when we compute the T_c of the transition element Nb . Then from (156) we can compute the highest critical temperature T_c of $La_{2-x}Sr_xCuO_4$:

$$T_c \approx 34.95K \quad (\text{Computed value of } T_c \text{ of } La_{2-x}Sr_xCuO_4) \quad (157)$$

This agrees with the experimental value of $T_c \approx 35K$ of $La_{2-x}Sr_xCuO_4$ at the optimal doping $x \approx 0.15$.

In a $La(Sr)O$ plane we have that one O atom can interact with two $La(Sr)$ atoms. This gives an interaction between two $La(Sr)$ atoms. With this additional interaction we have that the seagull vertex interaction gives the attractive effect for the forming of the Cooper pair of s valence electrons where the La atom is with outer shells $5d^16s^2$ and the Sr atom is with outer shell $6s^2$. The two s valence electrons for the forming of Cooper pair are with wave factors $e^{\pm ih_{La(Sr)}}$ respectively in their wave functions where $|h_{La(Sr)}|$ is the energy of the s electrons for the interaction of forming the Cooper pair. Then the Cu atom and the two $La(Sr)$ atoms on the centered c -axis of $La_{2-x}Sr_xCuO_4$ are regarded as a clustering of atoms and are regarded as a larger atom. Thus in the case of the appearing of Cooper ss -pairs of $La(Sr)$ atoms we have that the total energy gap of this clustering of atoms is $\Delta_{LSCO} = h = 5|h_{Cu}| + 2|h_{La(Sr)}|$. Then since a $La(Sr)$ atom in a $La(Sr)O$ plane can interact with only one O atom at the outside of this $La(Sr)O$ plane and next to this $La(Sr)$ atom we have that the s valence electrons of $La(Sr)$ can have at most two states of ionization energies. Thus the maximum value of the energy parameter $|h_{La(Sr)}|$ is proportional to the second ionization energy of La (or Sr). From the existing table of ionization energies we have that the second ionization energy of La is approximately equal to 1067 kJ/mol (The second ionization energy of Sr is approximately equal to 1064.2 kJ/mol and can be regarded as equal to that of the La atom). Let $|h_{La(Sr)}| \approx \xi 1067$ kJ/mol. Then from (156), with $\Delta_{LSCO} = 5|h_{Cu}| + 2|h_{La(Sr)}|$, we can compute the highest critical temperature T_c of $La_{2-x}Sr_xCuO_4$:

$$T_c \approx 39.14K \quad (\text{Computed } T_c \text{ of } La_{2-x}Sr_xCuO_4) \quad (158)$$

This agrees with another experimental value of $T_c \approx 39K$ of $La_{2-x}Sr_xCuO_4$ at the optimal doping $x \approx 0.15$. Thus from this high- T_c theory of superconductivity we can explain the two experimental values of T_c of $La_{2-x}Sr_xCuO_4$.

Let us investigate in more detail the mechanism of doping giving the high- T_c superconductivity. To this end we investigate the mechanism of the increasing of the doping parameter x giving the increasing of h for $La_{2-x}Sr_xCuO_4$.

Let us consider the following function:

$$f(x) = 1850.3(1 - \frac{x}{2}) + 4138\frac{x}{2} \quad (159)$$

where 1850.3 kJ/mol and 4138 kJ/mol are approximately the third ionization energies of La and Sr respectively. Since $1850.3 < 4138$ and h is proportional to the ionization energy we have that this function gives the relation that the increasing of x giving the increasing of h for $La_{2-x}Sr_xCuO_4$.

We have $1850.3 < 1957.9 < 4138$ where 1957.9 kJ/mol is the state of second ionization energy of Cu . Let us establish the following relation (A main point of this relation is that $1957.9 - 1850.3$ is small and $4138 > 1957.9$):

$$f(x_0) = 1850.3\left(1 - \frac{x_0}{2}\right) + 4138\frac{x_0}{2} = 1957.9 \quad (160)$$

for some x_0 ($0 < x_0 < 1$). This then relates the state of third ionization energy of La and the state of second ionization energy of Cu . When this relation holds (or approximately holds) we identify the case that the channel for the high- T_c superconductivity given by the CuO_2 plane is open. This channel opening gives a freedom of electric current with a direction orthogonal to the CuO_2 plane. From this freedom of electric current, the Cooper pairs of d valence electrons of Cu can be formed (In other words, through this channel opening the d valence electrons of Cu can transit from the valence band to the conduction band from which Cooper pairs of these d valence electrons can be formed). Thus this channel opening together with the CuO_2 plane gives the region of 3D superconductivity. From this region of 3D superconductivity we have the existence of quasi-2D bifurcation region of the unconventional high- T_c superconductivity given by the CuO_2 plane.

We notice that $x_0 \approx 0.094$. Thus the doping range $x_0 < x < x_1$ for some $x_1 < 1$ is a range for the state of high- T_c superconductivity. This agrees with the experiment that the state of high- T_c superconductivity of $La_{2-x}Sr_xCuO_4$ is in the doping range $0.06 \leq x \leq 0.3$. When (160) holds we have that the d valence electrons of Cu (forming Cooper pairs) are in the basic state of second ionization energy, and other states are to be reached from this basic state. Also when (160) holds the d valence electrons of Cu and $La(Sr)$ are unified to occupy the sequence of state of ionization energies. Since the Cu atoms in the CuO_2 plane are with one more ionization direction than the $La(Sr)$ atoms in the $La(Sr)O$ plane we have that the d valence electrons of Cu occupy the higher states while the d valence electrons of $La(Sr)$ occupy the lower states.

Then since there are no d valence electrons of $La(Sr)$ forming Cooper pairs and the d valence electrons of Cu have three states of ionization energies we have that the d valence electrons of Cu (forming Cooper pairs) have the states of first, second and third ionization energies. Thus the maximum value of the energy parameter $|h_{Cu}|$ is proportional to the third ionization energy of Cu . This gives a more detail explanation for that the energy parameter $|h_{Cu}|$ of the d valence electrons of Cu in $La_{2-x}Sr_xCuO_4$ is proportional to the third ionization energy of Cu .

16.5 Computation of T_c of $YBa_2Cu_3O_7$

Let us then investigate the mechanism of the high- T_c superconductivity of the cuprate $YBa_2Cu_3O_{6+x}$ ($0 \leq x \leq 1$). Similar to $La_{2-x}Sr_xCuO_4$ let us consider again the Cooper pairs of electrons of Cu as a mechanism for reducing h^2 to reach the state $\kappa^2 = 3h^2$ of superconductivity. As $La_{2-x}Sr_xCuO_4$, we consider the d valence electrons in the outer shells of valence electrons of Cu . It is known that $YBa_2Cu_3O_{6+x}$ has the multi-layer form $BaO/CuO/BaO/CuO_2/Y/CuO_2/BaO$ [46]. The two CuO_2 planes, one Y plane and one CuO plane are as a quantum system. The BaO planes are as external to this quantum system. Let us suppose that the multi-layer $CuO/BaO/CuO_2/Y/CuO_2$ can still be regarded as a quasi 2D system such that the above theory of high- T_c superconductivity can be applied. In this case the three Cu atoms at the (centered) c -axis of (a unit cell) joining the two CuO_2 planes and the CuO plane in the multi-layer $CuO/BaO/CuO_2/Y/CuO_2$ form a cluster. Thus the three Cu atoms can be regarded as a larger atom.

Let us first consider the CuO_2 planes. In a CuO_2 plane one Cu atom can interact with two O atoms. This gives an interaction between two Cu atoms. With this additional interaction we have that the seagull vertex interaction gives the attractive effect for the forming of the Cooper pair of d electrons. As $La_{2-x}Sr_xCuO_4$, the two d electrons for the forming of Cooper pair are with the wave factors $e^{\pm ih_{Cu}}$ respectively in their wave functions where $|h_{Cu}|$ is the energy of the d electrons for the interaction of forming the Cooper pair. Further since the two CuO_2 planes are separated by a Y plane there is only one direction of ionization orthogonal to the two CuO_2 planes we have that the d valence electrons of Cu of these two CuO_2 planes have only two states of ionization energies. We shall show that the maximum value

of the energy parameter $|h_{Cu}|$ of the d valence electrons of Cu of these two CuO_2 planes is proportional to the third ionization energy of Cu .

Let us then consider the CuO plane. In the CuO plane one O atom can interact with two Cu atoms in chain form. This gives an interaction between two Cu atoms. With this additional interaction we have that the seagull vertex interaction gives the attractive effect for the forming of the Cooper pair of d electrons. The two d electrons for the forming of Cooper pair are with wave factors $e^{\pm ih_{CuO}}$ respectively in their wave functions where $|h_{CuO}|$ is the energy of the d electrons for the interaction of forming the Cooper pair in the CuO plane. This energy parameter $|h_{CuO}|$ gives a wave factor $e^{i(h_{CuO}-h_{CuO})}$ of the Cooper pair of d electrons of Cu in the CuO plane. This cancelation of energy for the forming of Cooper pair gives the reduction of the energies of the Cu atoms. Thus the forming of Cooper pair of d electrons of Cu in the CuO plane is a mechanism for the reduction of energy. Since there is only one direction of ionization orthogonal to the CuO plane we have that the d valence electrons of Cu of the CuO plane have only two states of ionization energies. We shall show that the maximum value of the energy parameter $|h_{CuO}|$ of the d valence electrons of Cu in the CuO plane is proportional to the second ionization energy parameter of Cu . For the doping mechanism of superconductivity, let us consider the following function:

$$f(x) = 1980 - 3600(1 - x) \quad (161)$$

where 1980 kJ/mol and 3600 kJ/mol are the third ionization energies of Y and Ba respectively. This function gives the relation that the increasing of x giving the increasing of h ($0 \leq x \leq 1$). Then let us set up the following relation (A main point for setting up this relation is that $1980 - 1957.9$ is small and $3600 > 1980$):

$$f(x_0) = 1980 - 3600(1 - x_0) = 1957.9x_0 \quad (162)$$

for some x_0 ($0 < x_0 < 1$). Equivalently we have the following relation:

$$1980 = 1957.9x_0 + 3600(1 - x_0) \quad (163)$$

When this relation (162) holds (or approximately holds), the channel connecting the two states of second ionization energy of Cu and Y can be opened. This channel opening gives a freedom of electric current with a direction orthogonal to the two CuO_2 planes. From this freedom of electric current, the Cooper pairs of the $3d$ -level electrons of Cu can be formed. Thus this channel opening gives the 3D region of conventional superconductivity. From this 3D conventional superconductivity we have the existence of quasi-2D bifurcation region of unconventional high- T_c superconductivity given by the two CuO_2 planes. We notice that $x_0 \approx 0.9865$. Thus the cuprate $YBa_2Cu_3O_{6+x}$ comes into the range of high- T_c superconductivity when x is just greater than x_0 . Since $1 - x_0$ is very small we have that $x_c \approx 1$ is the optimal doping with highest T_c of high- T_c superconductivity. This agrees with the experiment that the cuprate $YBa_2Cu_3O_7$ is in optimal doping with highest T_c of high- T_c superconductivity.

When (162) holds, the d valence electrons of Cu in the CuO plane and the two CuO_2 planes are in the basic state of second ionization energy, and other states are to be reached from this basic state. Also when (162) holds the d valence electrons of Cu in the CuO plane and the two CuO_2 planes are unified to occupy the sequence of state of ionization energies. Since the Cu and O are interacted in chain form in the CuO plane we have that the Cu atoms in the CuO_2 plane are with one more ionization direction than the Cu atoms in the CuO plane. Thus the d valence electrons of Cu in the CuO_2 planes occupy the higher states of ionization energies while the d valence electrons of the Cu atoms in the CuO plane occupy the lower states. Thus the d valence electrons of Cu in the CuO_2 planes have the states of second and third ionization energies and the d valence electrons of Cu in the CuO plane have the state of first and second ionization energies. Thus the maximum value of the energy parameter $|h_{CuO}|$ of the d valence electrons of Cu in the CuO plane is proportional to the second ionization energy of Cu and the maximum value of the energy parameter $|h_{Cu}|$ of the d valence electrons of Cu in the two CuO_2 planes is proportional to the third ionization energy of Cu . Then we have the following formula of T_c of $YBa_2Cu_3O_{6+x}$:

$$k_B T_c = \kappa = \frac{1}{\sqrt{3}} \Delta_{YBCO} \quad (164)$$

where $\Delta_{YBCO} = h = 10|h_{Cu}| + 5|h_{CuO}|$ is the energy gap of $YBa_2Cu_3O_{6+x}$, where $10 = \frac{20}{2}$ is from the 20 d -electrons of two Cu atoms of two CuO_2 plane and $5 = \frac{10}{2}$ is from the 10 d -electrons of one Cu atom of the CuO plane of a unit cell of $YBa_2Cu_3O_{6+x}$. Then from the table of ionization energy, the second and third ionization energies of Cu are approximately equal to 1957.9 kJ/mol and 3555 kJ/mol. Let $|h_{Cu}| \approx \xi 3555$ kJ/mol and $|h_{CuO}| \approx \xi 1957.9$ kJ/mol. Then from (164) we can compute the highest critical temperature T_c of $YBa_2Cu_3O_{6+x}$:

$$T_c \approx 89.14K \quad (\text{Computed value of } T_c \text{ of } YBa_2Cu_3O_{6+x}) \quad (165)$$

This agrees with the experimental value of $T_c \approx 90K$ of $YBa_2Cu_3O_{6+x}$ [46].

Similar to the La atom for $La_{2-x}Sr_xCuO_4$, when the channel through Y is open, and the s valence electrons of Y also form a Cooper ss -pair, then this gives an energy parameter $|h_Y|$ which is proportional to the first ionization energy of Y . Then $\Delta_{YBCO} = h = 10|h_{Cu}| + 5|h_{CuO}| + |h_Y|$ where $|h_Y| \approx \xi 600$ kJ/mol (600 kJ/mol is approximately the first ionization energy of Y). Then from (164) we have:

$$T_c \approx 90.32K \quad (\text{Computed value of } T_c \text{ of } YBa_2Cu_3O_{6+x}) \quad (166)$$

This also agrees with the experimental value of $T_c \approx 90K$ of $YBa_2Cu_3O_{6+x}$ [46].

16.6 Computation of T_c of MgB_2

The intermetallic material MgB_2 is found to have the phenomenon of two-gap superconductivity [47, 56, 57, 58, 59, 60, 61]. Let us show that this phenomenon can also be derived from the above theory of high- T_c superconductivity. This material MgB_2 has two layers consisting of Mg and B respectively. It is known that MgB_2 has a structure that the B atoms in a layer of B form a honeycomb. Then each Mg atom in the layer of Mg is located in the center of each hexagon of the honeycomb. Thus a hexagon of six B atoms is enclosed by a hexagon of six Mg atoms and is separated from other hexagons of B atoms by the hexagon of six Mg atoms. Let us call such a hexagon of six B atoms as a unit element in a layer of B atoms.

The two s -valence electrons and the two s -electrons of the inner shell of a B atom give an energy $2|h_{B1}| + 2|h_{B2}|$. Then since the B atoms of a unit element are clustered together that these B atoms can be regarded as a larger atom. Thus the total s -electrons of a unit element of B atoms give the total energy $12|h_{B1}| + 12|h_{B2}|$. Let us consider the intermetallic $Mg_{1-x}Be_xB_2$ ($0 \leq x \leq 1$). This intermetallic is of the AlB_2 -type. For the doping mechanism of giving superconductivity, let us consider consider the following function:

$$f(x) = 737.7(1 - x) + 899.5x \quad (167)$$

where 737.7 kJ/mol and 899.5 kJ/mol are approximately the first ionization energies of Mg and Be respectively. Since $737.7 < 899.5$ and h is proportional to the ionization energy we have that this function gives the relation that the increasing of x giving the increasing of h for $Mg_{1-x}Be_xB_2$. We have $737.7 < 800.6 < 899.5$ where 800.6 kJ/mol is the first ionization energy of B . Let us set:

$$f(x_0) = 737.7(1 - x_0) + 899.5x_0 = 800.6 \quad (168)$$

for some x_0 ($0 \leq x_0 \leq 1$).

When this relation holds (or approximately holds), the channel connecting the two states of first ionization energy of B and Mg is open. This channel opening gives a freedom of electric current with a direction orthogonal to the B plane. By this freedom of electric current, the electrons of a cluster of atoms in a unit cell can be coupled to the electrons of other clusters to form Cooper pairs. In this way the Cooper pairs of s -valence (and nonvalence) electrons of B , the Cooper pairs of s -valence electrons of Mg can be formed. Thus this channel opening gives the 3D region (π -band) of conventional superconductivity. From this 3D conventional superconductivity we have the existence of quasi-2D bifurcation region (σ -band) of unconventional high- T_c superconductivity given by the B plane.

We notice that $x_0 \approx 0$. This agrees with the experiment that the state of superconductivity of $Mg_{1-x}Be_xB_2$ is in the doping range $0 \leq x < 1$ and that MgB_2 is in the state of superconductivity [62].

When (168) holds we have that the s valence electrons of B are in the state of first ionization energy of B . Then the s nonvalence electrons of B are in the state of second ionization energy of B . Also the s valence electrons of Mg are in the state of first ionization energy of Mg . The s valence electrons of B and Mg in the state of first ionization energy are in the opened channel of 3D superconductivity while the s nonvalence electrons of B in the state of second ionization energy of B are for the quasi-2D high- T_c superconductivity of the B plane. Thus the maximum value of the energy parameter $|h_{B1}|$ and $|h_{B2}|$ are proportional to the first and second ionization energies of B respectively, and the maximum value of the energy parameter $|h_{Mg}|$ of the s valence electrons of Mg is proportional to the first ionization energy of Mg . Then we have the following formula of T_c of MgB_2 :

$$k_B T_c = \kappa = D_{MgB_2} \Delta_{MgB_2} \quad (169)$$

where $\Delta_{MgB_2} = h = 6|h_{B1}| + 6|h_{B2}| + |h_{Mg}|$ is the energy gap of superconductivity of MgB_2 , where $6 = \frac{12}{2}$ is from the 12 valence or nonvalence s electrons of the B atoms in a hexagonal unit cell of MgB_2 . From the existing table of ionization energy of B , the first and second ionization energies of B are approximately equal to 800.6 kJ/mol and 2427.1 kJ/mol respectively. Let $|h_{B1}| \approx \xi 800.6$ kJ/mol and $|h_{B2}| \approx \xi 2427.1$ kJ/mol, $|h_{Mg}| \approx \xi 737.7$ kJ/mol. Thus from (169) we have:

$$T_c \approx 39.53K \quad (\text{Computed value of } T_c \text{ of } MgB_2) \quad (170)$$

This agrees with the experimental value of $T_c \approx 39K$ of MgB_2 [47].

We notice that the energy gap $\Delta_{MgB_2} = h = 6|h_{B1}| + 6|h_{B2}| + |h_{Mg}|$ contains the sum of two energy gaps $\Delta_1 = h = 6|h_{B1}|$ and $\Delta_2 = h = 6|h_{B2}|$. We have that Δ_1 correspond to the conventional 3D superconductivity while Δ_2 correspond to the unconventional quasi-2D superconductivity. In this case we have the phenomeon of two-gap superconductivity [47, 56, 57, 58, 59, 60, 61].

Then, from experiments we have two energy gaps: $\Delta_\sigma(4.2K) \approx 7.1meV$ and $\Delta_\pi(4.2K) \approx 2.3meV$ where Δ_σ is a 2D energy gap and Δ_π is a 3D energy gap [47, 56, 57, 58, 59, 60, 61]. Thus, Δ_σ corresponds to Δ_2 and Δ_π corresponds to Δ_1 . Thus we have:

$$\frac{\Delta_2}{\Delta_1} = \frac{2427.1}{800.6} \approx 3.03 \quad (\text{Computed value of } \frac{\Delta_\sigma(4.2K)}{\Delta_\pi(4.2K)}) \quad (171)$$

This agrees with the experimental value of $\frac{\Delta_\sigma(4.2K)}{\Delta_\pi(4.2K)} = \frac{7.1}{2.3} \approx 3.08$ [47, 56, 57, 58, 59, 60, 61].

17 Examples of conventional superconductors

Let us first consider the element Nb . This element is with the outer shells $4d^45s^1$ of valence electrons. Since Nb is a metal, Nb is in the state $\kappa^2 < \frac{1}{3}h^2$. For Nb in the state of superconductivity, h^2 is needed to be reduced such that $\kappa^2 \geq \frac{1}{(2+\sqrt{3})^2}h^2$. In this case we need a mechanism for the decreasing of h to reach the state of superconductivity. Let the Cooper pair be such a mechanism. Let the four d electrons be with the wave factor $e^{ih_{Nb}}$ where h_{Nb} is the energy of the d electrons. When the temperature T is low enough we have the phase transition of Bose-Einstein condensation. This phase transition is with the changing of the spin of two of d electrons such that the state of these two d electron are changed from the state $e^{ih_{Nb}}$ to the state $e^{-ih_{Nb}}$. Thus we have two Cooper pairs of d electrons. The forming of the Cooper pairs reduces the total energy $4|h_{Nb}|$ of the four d electrons of Nb to $2|h_{Nb}|$. Thus we have the following formula of T_c of Nb :

$$k_B T_c = \kappa = \frac{1}{\sqrt{3}} \Delta_{Nb} \quad (172)$$

where $\Delta_{Nb} = h = 2|h_{Nb}|$ is the energy gap of superconductivity of Nb . Let us then determine the energy $|h_{Nb}|$. As the case of high- T_c superconductivity, the d valence electrons of Nb can be in the state with the third ionization energy of Nb . From the existing table of ionization energies, the third ionization energy of Nb is approximately equal to 2416 kJ/mol. Let $|h_{Nb}| \approx \xi 2416$ kJ/mol where ξ is the proportional constant. Then from (172) let us compute the constant ξ by using the experimental value $T_c \approx 9.5K$:

$$k_B 9.5 = \kappa = \frac{1}{\sqrt{3}} \xi 2 \cdot 2416 \quad (173)$$

This gives $\xi \approx 2.83133971 \cdot 10^{-5}$. From this value of ξ , the computed T_c of Nb is equal to the experimental value $T_c = 9.5K$ of Nb . Since the superconductivity of Nb is from the d electrons this is as the Type II superconductivity.

Let us then consider the element Pb . This element is with the outer shell $6s^26p^2$ of valence electrons. Since Pb is a metal we have that Pb is in the state $\kappa^2 < \frac{1}{3}h^2$. Thus Pb is with the Cooper pair as the mechanism in reaching the state of superconductivity. There are two p valence electrons with the same spin and two s valence electrons with different spins. One of the two s electrons with the wave factor $e^{-ih_{Pb1}}$ is coupled with a s electron with wave factor $e^{ih_{Pb1}}$ of another atom Pb . When the temperature T is low enough the spin of one of the p valence electron is changed. Then one of the two p electrons with the wave factor $e^{-ih_{Pb2}}$ is coupled with a p electron with wave factor $e^{ih_{Pb2}}$ of another atom Pb . This forms a Cooper pp -pair. This gives a reduction of energy. Because the pp -pairing is obtained by changing the spin of a p electron, as the case of Nb , the energy parameter h_{Pb2} is proportional to the third ionization energy of Pb . In this case this is a Type I superconductivity because this is a pp -pairing. Then the forming of the two Cooper pairs reduces the total energy $2|h_{Pb1}| + 2|h_{Pb2}|$ of the two s electrons and the two p electrons for forming the two Cooper pairs. Then we have the following formula of critical temperature T_c of Pb :

$$k_B T_c = \kappa = \frac{1}{\sqrt{3}} \Delta_{Pb} \quad (174)$$

where $\Delta_{Pb} = h = |h_{Pb1}| + |h_{Pb2}|$ is the energy gap of superconductivity of Pb . Then from the existing table of ionization energies, the first and third ionization energies of Pb are approximately equal to 715.6 kJ/mol and 3081.5 kJ/mol respectively. Let $|h_{Pb1}| \approx \xi 715.6$ kJ/mol and $|h_{Pb2}| \approx \xi 3081.5$ kJ/mol. Then from (174) we can compute the critical temperature T_c of Pb :

$$T_c \approx 7.463K \quad (\text{Computed value of } T_c \text{ of } Pb) \quad (175)$$

This agrees with the experimental value of $T_c \approx 7.193K$ of Pb .

18 Superfluid and color superconductivity in neutron star

In the phase of quark-gluon-plasma (QGP) of neutrons and protons, it is argued that there are pairing mechanisms of flavor quarks and color quarks for the states of superfluid and superconductivity of flavor quarks and color quarks [63]. In the literature the possible state of superconductivity of quarks is usually called the color superconductivity of quarks since the existing theory of the strong interaction of quarks is the QCD theory [63].

In this section let us use the above renormalization group analysis to investigate the states of superfluid and superconductivity of quarks in the core of neutron star where the neutrons and protons are in the phase of QGP.

In the phase of QGP of neutrons and protons, since quarks are still confined by the quantum knots of protons and neutrons, each neutron or proton can be regarded as a unit cell of the condensed matter QGP of neutrons and protons, just as the crystal unit cell of metals. Then since there are three (more than two) quarks and two quarks with up and down spins in a neutron or a proton which are as a unit cell of a crystal, it is possible to form Cooper pairs of quarks between two neutrons or two protons.

In the above section on renormalization group equations we have shown that QCD has two nontrivial fixed points. Since QCD has two nontrivial fixed points, there are two special phase lines \mathbf{e} . Thus the region for the forming of the quasi-2D phase of superconductivity (or superfluid) of one nontrivial fixed point overlaps with the region of 3D phase of superconductivity (or superfluid) of another nontrivial fixed point in the phase diagram of QGP. Thus the quasi-2D phase of superconductivity always exists stably in the case of the existence of the 3D phase of superconductivity (or superfluid). This also means that there are layers of quasi-2D dimensional superconducting protons (or quasi-2D dimensional superfluid of neutrons).

Since the quasi-2D phase of superconductivity (or superfluid) can stably exist, this gives that the color superconductivity (or superfluid) can exist with no upper limit on the critical temperature T_c . This

agrees with the recent analysis of data of cooling rate of the neutron star of Cassiopeia A (Cas A) that the critical temperature T_c is very high that $T_c \geq 2 \times 10^9 K$ [64][65].

Further, since protons are of about 10 percent in the neutron star of Cas A, protons may form layers in the neutron star of Cas A. Then the quarks of neutrons and of the protons are approximately with the same ionization energies (or the energy of the nearly free of the quarks), we have that a channel opening between neutron and proton is possible at some energy of the nearly free of quarks. Thus 3D superfluid of quarks of neutrons near the layers of protons and quasi-2D superconductivity of quarks of the layers of protons both exist and this gives the quasi-2D high- T_c superconductivity of quarks of protons. Then since the energy of the nearly free of the quarks is very high that the critical temperature T_c is very high by the formula of T_c as that in the QED case. In the forming of pairing of quarks of protons, energy is not released in the neutrino form and the neutron star is not cooled by the energy released in the neutrino form.

Then more and more quarks of neutrons form the 3D superfluid through the channel opening while the quasi-2D superconductivity of quarks of the layers of protons exists. In the pairing of quarks of neutrons in forming the 3D superfluid, energy is released in the neutrino form and the neutron star is cooled. This is as the period of rapidly cooling rate of the neutron star of Cas A. This gives the superfluid and color superconductivity in the core of the neutron star of Cas A.

References

- [1] E. Witten, Quantum field theory and the Jones polynomial, *Commun. Math. Phys.* **121**, 351 (1989)
- [2] P.A.M. Dirac, *Directions in Physics*, (John Wiley, 1978).
- [3] C. Itzykson and J-B. Zuber, *Quantum Field Theory*, (McGraw-Hill Inc., 1980).
- [4] L. Kauffman, *Knots and Physics*, (World Scientific 1993).
- [5] J. Baez and J. Muniain, *Gauge Fields, Knots and Gravity*, (World Scientific 1994).
- [6] V. Chari and A. Pressley, *A Guide to Quantum Groups*, (Cambridge University Press 1994).
- [7] T. Kohno, *Ann. Inst. Fourier (Grenoble)* **37** 139-160 (1987).
- [8] V. G. Drinfel'd, *Leningrad Math. J.* **1** 1419-57 (1990).
- [9] S.K. Ng, arXiv hep-th/0209143v6.
- [10] P. Di Francesco, P. Mathieu and D. Senechal, *Conformal Field Theory*, (Springer-Verlag 1997).
- [11] J. Fuchs, *Affine Lie Algebras and Quantum Groups*, (Cambridge University Press 1992).
- [12] V.G. Knizhnik and A.B. Zamolodchikov, Current algebra and Wess-Zumino model in two dimensions, *Nucl. Phys. B* **247**, 83 (1984).
- [13] K. Murasugi, *Knot Theory and Its Applications*, (Birkhauser Verlag, 1997).
- [14] W.B.R. Lickorish, *An Introduction to Knot Theory*, (Springer, 1997).
- [15] S.K. Ng, arXiv hep-th/0210024v4.
- [16] K.G. Wilson and M.E. Fisher, *Phys. Rev. Lett.*, **28**, p.248 (1972).
- [17] K. Huang, *Statistical Mechanics*, John Wiley and Sons, 1987.
- [18] L.Yu and B. Hao, *Advances in Statistical Physics (in Chinese)*, Science Press, 1981.
- [19] R.J. Creswick, H.A. Farach and C.P. JR. Poole, *Introduction to Renormalization Group Methods in Physics*, John Wiley and Sons, 1992.

- [20] L. Onsager, *Phys. Rev.*, **65**, p.117 (1944).
- [21] J. Bardeen, L.N. Cooper and J.R. Schrieffer, *Phys. Rev.*, **108**, 1175 (1957).
- [22] A.A. Abrikosov, *Sov. Phys. JETP*, **5**, 1174 (1957).
- [23] N.N. Bogoliubov, *Sov. Phys. JETP*, **7**, 41 (1959).
- [24] J. Hubbard, *Proc. Roy. Soc. London Ser. A*, **276**, 238 (1963).
- [25] L.P. Gor'kov, *Zh. Eksp, Teor. Fiz.*, **36**, 1364 (1986).
- [26] M.Tinkham, Introduction to superconductivity, McGraw-Hill, 1975.
- [27] L.P. Levy, *et al. Phys. Rev. Lett.*, **64**, 2074 (1990).
- [28] V. Chandrasekhar, *et al. Phys. Rev. Lett.*, **67**, 3578 (1991).
- [29] D. Mailly, *et al. Phys. Rev. Lett.*, **70**, 2020 (1993).
- [30] H. Bary-Soroker, *et al. Phys. Rev. Lett.*, **101**, 057001 (2008).
- [31] H. Bluhm, *et al. Phys. Rev. Lett.*, **102**, 36802 (2009).
- [32] D.J. Thompson, *et al., Phys. Rev. Lett.*, **75**, 529 (1995).
- [33] P. Kostic, *et al., Phys. Rev. B*, **53**, 791 (1996).
- [34] P. Svedlindh, *et al., Physica C*, **162**, 1365 (1989).
- [35] W. Braunsch, *et al., Phys. Rev. B*, **48**, 4030 (1993).
- [36] D. Khomskii, *et al., J. Low. Temp. Phys.*, **95**, 205 (1994).
- [37] M. Sigrist and T.M. Rice, *Rev. Mod. Phys.*, **67**, 503 (1995).
- [38] S. Riedling, *et al., Phys. Rev. B*, **49**, 13283 (1994).
- [39] W.D. Wise, *et al. Nature Physics*, **4**, 696 (2008).
- [40] O. Degtyareva, *et al., Phys. Rev. Lett.*, **99**, 155505 (2007).
- [41] E. Berg, *et al., Phys. Rev. Lett.*, **100**, 027003 (2008).
- [42] K. Seo, *et al., Phys. Rev. B*, **78**, 094510 (2008).
- [43] W.Y. Liang, *et al., J. Phys.: Condens. Matter*, **10**, 11365 (1998).
- [44] W. Braunsch, *et al., Phys. Rev. Lett.*, **68**, 1908 (1992).
- [45] T. Timusk and B. Statt, *Rep. Prog. Phys.*, **62**, 61 (1999).
- [46] M.K. Wu, *et al., Phys. Rev. Lett.* **58**, 908 (1987).
- [47] J. Nagamatsu, *et al., Nature*, **410**, 63 (2001).
- [48] J.M. Tranquada, *et al. Nature*, **375**, 561 (1995).
- [49] M. Fujita, *et al. Phys. Rev. B*, **70**, 104517 (2004).
- [50] N. Ichikawa, *et al. Phys. Rev. Lett.*, **85**, 1738 (2000).
- [51] V.J. Emery, S.A. Kivelson, and O. Zachar, *Phys. Rev. B*, **56**, 6120 (1997).

- [52] J. Zaanen, *et al. Phil. Mag, B*, **81**, 1485 (2001).
- [53] K. Machida, *Physica C*, **158**, 192 (1989).
- [54] A. Bianconi, *et al. Physica C: Superconductivity*, 341-348 (No. 1-4) , 1719-1722 (2000).
- [55] S.A. Kivelson, *et al. Rev. Mod. Phys.*, **75**, 1201 (2003).
- [56] X.K. Chan, *et al., Phys. Rev. Lett.*, **87**, 1570021 (2001).
- [57] A.Y. Liu, *et al., Phys. Rev. Lett.*, **87**, 0870051 (2001).
- [58] H.J. Choi, *et al., Nature*, **418**, 758 (2002).
- [59] M. Iavarone, *et al., Phys. Rev. Lett.*, **89**, 1870021 (2002).
- [60] F. Bouquet, *et al., Phys. Rev. Lett.*, **89**, 257001-1 (2002).
- [61] A.V. Sologubenko, *et al., Phys. Rev. B*, **66**, 014504 (2002).
- [62] I. Felner, cond-mat/0102508.
- [63] M.G. Alford, *et al., Rev. Mod. Phys.*, **80**, 1455 (2008).
- [64] D. Page, *et al., Phys. Rev. Lett.*, **106**, 081101 (2011).
- [65] P.S. Shternin, *et al., Not. R. Astron. Soc. Mon. Not. Roy. Astron. Soc. , 412*, L108-L112 (2011).